

THE REDISTRIBUTION OF RARE-EARTH ELEMENTS IN SECONDARY MINERALS OF HYDROTHERMAL VEINS, SCHWARZWALD, SOUTHWESTERN GERMANY

SUSANNE GÖB AND THOMAS WENZEL[§]

Fachbereich Geowissenschaften, Universität Tübingen, Wilhelmstrasse 56, D-72074 Tübingen, Germany

MICHAEL BAU

Earth & Space Sciences Program, Jacobs University Bremen, Campus Ring 1, D-28759 Bremen, Germany

DORRIT E. JACOB

Institut für Geowissenschaften and Earth System Science Research Centre, Johannes Gutenberg Universität, J.J. Becher-Weg 21, D-55099 Mainz, Germany

ANSELM LOGES AND GREGOR MARKL

Fachbereich Geowissenschaften, Universität Tübingen, Wilhelmstrasse 56, D-72074 Tübingen, Germany

ABSTRACT

Minerals of the rare-earth elements (REE) occur as supergene phases in the Schwarzwald ore district, southwestern Germany. They form by alteration of hydrothermal fluorite – barite – quartz – carbonate veins with various associations, including Cu–Pb, Pb–Zn and Co–Bi–Ag–U assemblages in sandstones, gneisses and granites. The REE minerals, including mixite-group minerals ($(\text{REE}, \text{Bi}, \text{Ca}, \text{Pb})\text{Cu}_6(\text{AsO}_4, \text{AsO}_3\text{OH})_3\text{OH}_6 \cdot 3\text{H}_2\text{O}$), rhabdophane and churchite ($\text{REEPO}_4 \cdot \text{H}_2\text{O}$ and $\text{REEPO}_4 \cdot 2\text{H}_2\text{O}$), chukhrovite ($\text{Ca}_3\text{REEAl}_2\text{SO}_4\text{F}_{13} \cdot 10\text{H}_2\text{O}$) and bastnäsite (REECO_3F), were analyzed by electron microprobe and LA–ICP–MS. In addition, REE concentrations in secondary fluorite, calcite and Mn oxides cogenetic with the REE minerals were determined by LA–ICP–MS. Results of analyses of 74 mixite-group samples from 20 localities in the Schwarzwald ore district show that continuous miscibility is possible between REE and Ca and between Bi and Ca end-members. In contrast, no miscibility seems to exist between the Bi and REE end-members, and only Ca-rich members can accommodate small amounts of both Bi and REE. The REE phosphates churchite and rhabdophane do not occur at the same locality in the Schwarzwald, which is probably dependent on which REE (light or heavy) predominate at a certain locality. Whereas churchite incorporates heavy REE (HREE), rhabdophane prefers light REE (LREE). Dependent on the source of the REE, either HREE or LREE dominate in an alteration fluid and, consequently, only one type of REE phosphate forms. The HREE dominate in such a fluid if REE originate from dissolved “pitchblende”, whereas the LREE dominate if the altered host-rock or dissolved fluorite are the source of the REE. The REE contents of Mn oxides and calcite cogenetic with REE-bearing mixite-group minerals show that the REE distribution of secondary minerals can be influenced by each other. Whereas the Mn oxides incorporate Ce^{4+} resulting in a positive Ce anomaly, a cogenetic mixite-group mineral develops a negative anomaly, which shows that Ce anomalies are coupled. Calcite intergrown with a mixite-group mineral can only incorporate those REE that are not consumed by the latter. These processes involve the distribution of REE between minerals on the micrometer scale and do not take place until minerals precipitate. However, sorption and complexation processes also take place during transport on a larger scale and produce decoupled Ce anomalies. This interplay between large- and small-scale processes results in a complex redistribution of REE during remobilization.

Keywords: rare-earth elements, agardite, mixite, rhabdophane, churchite, supergene alteration, remobilization, Schwarzwald, Germany.

SOMMAIRE

Les minéraux des terres rares sont présents comme phases supergènes dans le district minéralisé de la Forêt Noire, dans les sud-ouest de l'Allemagne. Ils se sont formés par altération de veines hydrothermales à fluorite – barite – quartz – carbonate dans des associations diverses, y inclus des assemblages à Cu–Pb, Pb–Zn et Co–Bi–Ag–U dans des grès, des

[§] E-mail address: markl@uni-tuebingen.de

gneiss et des granites. Nous avons analysé les minéraux de terres rares (TR), y inclus les minéraux du groupe de la mixite ($[\text{TR}, \text{Bi}, \text{Ca}, \text{Pb}] \text{Cu}_6(\text{AsO}_4, \text{AsO}_3\text{OH})_3\text{OH}_6 \cdot 3\text{H}_2\text{O}$), rhabdophane et churchite ($\text{TRPO}_4 \cdot \text{H}_2\text{O}$ et $\text{TRPO}_4 \cdot 2\text{H}_2\text{O}$), chukhrovite ($\text{Ca}_3\text{TRAl}_2\text{SO}_4\text{F}_{13} \cdot 10\text{H}_2\text{O}$) et bastnäsité (TRCO_3F), avec une microsonde électronique et par la méthode ICP-MS avec ablation au laser. De plus, la concentration des terres rares dans la fluorite secondaire, la calcite et des oxydes de Mn co-génétiques avec les minéraux de terres rares ont aussi été analysés par ablation au laser avec ICP-MS. Les compositions de 74 échantillons représentant le groupe de la mixite provenant de 20 localités dans ce district montrent une miscibilité complète entre les pôles à TR et à Ca, et entre les pôles à Bi et à Ca. En revanche, il n'y a aucune miscibilité entre les pôles à Bi et à TR, et seuls les membres riches en Ca peuvent accommoder de légères quantités de Bi et TR. La churchite et rhabdophane, phosphates de TR, ne coexistent pas dans ce district, et apparaissent probablement selon quel groupe, TR légères ou lourdes, prédomine dans un endroit donné. Tandis que la churchite incorpore les TR lourdes, la rhabdophane préfère les TR légères. Selon la source des TR, ce sont les TR lourdes ou légères qui prédominent dans une phase fluide causant l'altération, ce qui explique pourquoi seulement une sorte de phosphate de TR précipite. Les TR lourdes prédominent si c'est la "pechblende" qui est affectée; en revanche, les TR légères prédominent si c'est la roche hôte ou la fluorite qui est lessivée. Les teneurs en terres rares des oxydes de Mn et de la calcite co-génétiques avec les minéraux du groupe de la mixite montrent que les minéraux secondaires peuvent être mutuellement influencés dans leur distribution des TR. Tandis que les oxydes de Mn incorporent le Ce^{4+} , menant à une anomalie positive en Ce, un membre du groupe de la mixite co-génétique peut développer une anomalie négative en Ce; leurs anomalies seraient donc couplées. La calcite en intercroissance avec un membre du groupe de la mixite ne peut donc incorporer que les TR qui ne sont pas incorporées par le minéral coexistant. Ces processus impliquent la distribution des TR entre minéraux à une échelle micrométrique et fonctionnent lors de leur précipitation. Toutefois, les processus de sorption et de complexation seraient aussi importants au cours du transfert sur une plus grande échelle, et produisent des anomalies découplées en Ce. Cette interaction entre processus à longue ou à courte échelle rend compte de la redistribution complexe des TR au cours de leur remobilisation.

(Traduit par la Rédaction)

Mots-clés: terres rares, agardite, mixite, rhabdophane, churchite, alteration supergène, remobilisation, Schwarzwald, Allemagne.

INTRODUCTION

In the Schwarzwald ore district, southwestern Germany, minerals of the rare-earth elements (REE) are commonly developed as secondary supergene phases in hydrothermal veins (*e.g.*, Walenta 1992). They comprise mixite-group minerals, bastnäsité, rhabdophane, churchite and chukhrovite, which typically grow as secondary euhedral or needle-shaped crystals in vugs. Other REE minerals like florencite, fluocerite, monazite, synchysite or xenotime occur as well (Walenta 1992), but are too rare and their crystals too tiny to be incorporated into the present study. Here, we present the first comprehensive district-scale study of both the mineralogy and mineral assemblages, and the quantitative composition of REE minerals. In addition, associated REE-bearing fluids (mine waters) and solid phases such as fluorite, calcite and Mn oxides were investigated. On the basis of this dataset, we draw conclusions about processes of REE remobilization in hydrothermal veins in the deposits of the Schwarzwald ore district by combining information on both REE mineral assemblages and the details of REE compositional variations in cogenetic solid phases and fluids.

BACKGROUND INFORMATION

The REE occur only as trace elements in most rock-forming minerals, but can be highly concentrated in minerals like rhabdophane ($\text{REEPO}_4 \cdot \text{H}_2\text{O}$), churchite ($\text{REEPO}_4 \cdot 2\text{H}_2\text{O}$), bastnäsité (REECO_3F), mixite-group minerals [$\text{REECu}_6(\text{AsO}_4)_3\text{OH}_6 \cdot 3\text{H}_2\text{O}$] or chukhro-

vite ($\text{Ca}_3\text{REEAl}_2\text{SO}_4\text{F}_{13} \cdot 10\text{H}_2\text{O}$). Those minerals commonly occur as alteration products in crystalline rocks (Berger *et al.* 2008, Krenn & Finger 2007, Nagy *et al.* 2002, Nagy & Draganits 1999, Lottermoser 1990) or in the oxidation zone of ore deposits (Dietrich *et al.* 1969, Walenta 1979, 1982).

Mixite-group minerals are a group of Cu arsenates with the general formula $M1M2_6(\text{XO}_4)_3\text{OH}_6 \cdot 3\text{H}_2\text{O}$ with *M1* representing REE, Bi, Ca, Pb and Al, *M2* representing Cu, and *X* stands for As and P. Known arsenate end-members are agardite (REE), mixite *sensu stricto* (Bi), zálesíte (Ca), plumboagardite (Pb), and goudeyite (Al) (Table 1, references therein). The REE-bearing phosphate analogue is petersite. Several previous studies on mixite-group minerals exist: Dietrich *et al.* (1969) qualitatively analyzed thirty-one mixite-group minerals from different localities worldwide and found samples containing either Bi or REE. Walenta (1960, 1970,

TABLE 1. END MEMBERS OF THE MIXITE GROUP OF MINERALS

end member	M1	M2 ₆	X	X2	OH ⁻	H ₂ O
agardite ^a	REE	Cu ₆	AsO ₄	(AsO ₄) ₂	(OH) ₆	3H ₂ O
zálesíte ^b	Ca	Cu ₆	AsO ₃ OH	(AsO ₄) ₂	(OH) ₆	3H ₂ O
mixite ^c	Bi	Cu ₆	AsO ₄	(AsO ₄) ₂	(OH) ₆	3H ₂ O
petersite ^d	REE	Cu ₆	PO ₄	(PO ₄) ₂	(OH) ₆	3H ₂ O
goudeyite ^e	Al	Cu ₆	AsO ₄	(AsO ₄) ₂	(OH) ₆	3H ₂ O
plumboagardite ^f	Pb	Cu ₆	AsO ₃ OH	(AsO ₄) ₂	(OH) ₆	3H ₂ O

^a Dietrich *et al.* (1969), ^b Sejkora *et al.* (1999), ^c Schrauf (1880), ^d Peacor & Dunn (1982), ^e Wise (1978), ^f Walenta & Theye (2005).

2003, 2004) and Walenta & Theye (2005) examined various mixite-group minerals from the Schwarzwald ore district using energy-dispersive electron-microprobe analyses (EDX), but the REE quantification in some of these publications has to be regarded with caution (see below). Information concerning the precise chemical composition and miscibility between end members of natural mixite-group minerals is sparse (Aruga & Nakai 1985, Olmi *et al.* 1991, Sejkora *et al.* 1999, Miyawaki *et al.* 2000, Kunov *et al.* 2002, de Baranda *et al.* 2003, Frost *et al.* 2005a, Tanaka *et al.* 2009). Most of these publications contain analytical data on single minerals. In addition to studies on natural samples, experimental studies on synthetic mixite-group minerals were published by Miletich & Zemann (1993) and Miletich *et al.* (1997), who studied the reversible hydration behavior involving zeolitic water in synthetic mixite. Further dehydration studies and Raman spectroscopic analyses were done by Frost *et al.* (2004, 2005b, 2005c).

Rhabdophane and churchite (or "weinschenkite") are REE phosphates containing different amounts of molecular H₂O (REEPO₄•H₂O and REEPO₄•2H₂O). Whereas rhabdophane prefers light REE (LREE), churchite favors Y and the heavy REE (HREE; Hikichi *et al.* 1978, 1989) and is invariably Y-dominant. Re-analysis of suspected Dy-dominant churchite (Walenta 1989) proved to be churchite-Y as well (Walenta & Theye 2011). The hydrous phosphates can transform into the anhydrous structures, *i.e.*, monazite and xenotime at 500 and 300°C, respectively (Hikichi *et al.* 1989).

Chukhrovite is a rare mineral reported only from five localities worldwide, among them Kara-Oba, Kazakhstan (including quantitative analyses; Pautov *et al.* 2005) and the Clara mine in the Schwarzwald (qualitative analyses only; Walenta 1979). Bastnäsite occurs in magmatic rocks, especially carbonatites (*e.g.*, Zambezi *et al.* 1997), but also forms as an alteration product in granitic rocks (Berger *et al.* 2008).

Several common minerals in the REE-mineral-bearing hydrothermal veins contain trace amounts of REE. Some of these minerals, for example fluorite, Mn oxides or calcite, are cogenetic with the REE minerals; others are primary and hence older phases. The most important of the latter is hydrothermal fluorite (REE in the ppm range; Schwinn & Markl 2005). Fluorite compositions from the whole Schwarzwald compared to compositional data on water from gneiss and granite aquifers show that REE in fluorite allow one to discriminate between sources from gneiss or granitic host-rocks (Schwinn & Markl 2005, Möller *et al.* 1997). Circulating oxidized fluids lead to element remobilization and to the formation of a wealth of secondary minerals in the veins (Walenta 1992, Hofmann & Eikenberg 1991, Markl & Bucher 1997, Markl *et al.* 2006). Besides different REE minerals, secondary fluorite, calcite and Fe and Mn oxides are the most notable minerals in terms of modifying and understanding REE distributions in low-temperature fluids. All these

phases contain REE, which makes them suitable for reconstruction of remobilization processes. Secondary fluorite differs from primary fluorite in displaying a negative Ce anomaly (Schwinn & Markl 2005, Loges *et al.* 2009, Staude *et al.* in press).

GEOLOGICAL SETTING

The Schwarzwald ore district, southwestern Germany (Fig. 1), is part of the Central European Variscides. Its crystalline basement is mainly composed of gneisses, migmatites and granites (Geyer & Gwinner 1986, Kalt *et al.* 2000). To the east, the basement is overlain by sandstones and limestones of Triassic to Jurassic age. In the west, the Schwarzwald is bounded by the Upper Rhine graben (URG).

The crystalline basement, as well as parts of the sedimentary cover, host more than 1000 hydrothermal veins (Metz *et al.* 1957, Bliedtner & Martin 1986). These veins contain fluorite, barite, quartz and calcite as gangue minerals and various Pb, Zn, Cu, Bi, Ag, U and Co ores. Detailed studies have focused on conditions of vein formation including dating (Pfaff *et al.* 2009) and precipitation mechanisms (Baatartsovt *et al.* 2007, Staude *et al.* 2007, Pfaff *et al.* 2010). Five types of veins can be distinguished by their age, genesis, geochemistry and mineralogy (Staude *et al.* 2009). These are (1) Permian quartz veins with Sb–Ag(–Au) mineralization, (2) Jurassic quartz – fluorite – barite veins with Fe–Mn, U–Bi–Ag–Co–Ni or Pb–Zn–Cu mineralization, (3) Paleogene quartz–barite veins with galena mineralization related to the opening of the URG, (4) Miocene barite veins with emplectite and Bi-bearing tennantite in the northern Schwarzwald, and (5) fluorite–barite veins around Wolfach and Haslach with Pb–Zn–Ag mineralization of unknown age. Veins that have not been classified are carbonate veins with Cu mineralization, hydrothermal quartz veins with W–Bi–Cu–As mineralization formed by late-magmatic fluids of Variscan granites (Werner *et al.* 1990, Schatz & Otto 1989), and the granite-hosted U deposit at Menzenschwand in the southern Schwarzwald, which formed from hydrothermal fluids in the Upper Carboniferous, with remobilization in Jurassic and Tertiary times (Hofmann 1989).

DESCRIPTION OF THE SAMPLES

Solid phases

The samples of REE minerals described here originate from various localities from all over the Schwarzwald (Fig. 1, Table 2). Localities in the northern Schwarzwald are barite–quartz veins or fluorite veins hosted by granites and sandstones (Staude *et al.* 2009), which are partly overlain by limestones. Along the Northern Kinzigtal Fault (NKF), veins with Cu–Pb–Ag mineralization are hosted by gneisses (Staude *et al.*

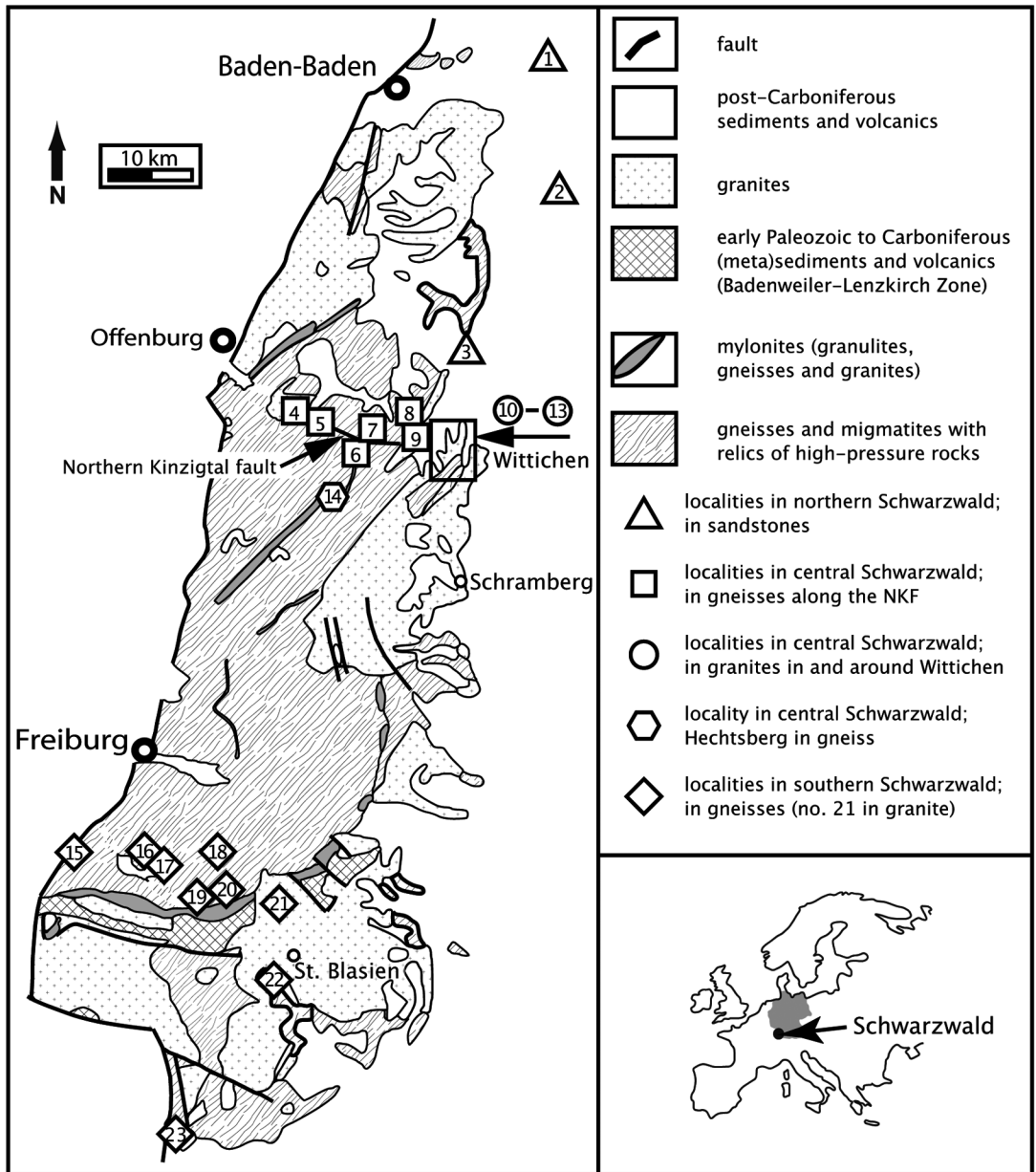


FIG. 1. Geological map of the Schwarzwald, modified after Kalt *et al.* (2000), with major geological units and sample localities.

2009, 2010a). Fluorite–barite veins in Wittichen are hosted by granites, and the Co–Bi–Ag–U mineralization in this area is unique in the Schwarzwald (Stauda *et al.*, in press). The Hechtsberg quarry is known for its Co–Cu–As–Ag mineralization in gneisses without pronounced hydrothermal veins (Otto 1974, Krause *et al.* 1997). Localities in the southern Schwarzwald are

more diverse. Most veins are fluorite–barite-bearing with Pb–Zn ores in gneisses (Metz *et al.* 1957). However, Amalie near Grunern is a barite–quartz vein with a tennantite–tetrahedrite–galena mineralization; the veins of Rotenbach–Feldberg are carbonate-bearing with chalcopyrite and tetrahedrite–tennantite. Säckingen in the southern Schwarzwald, formed by late-

TABLE 2. CLASSIFICATION AND DESCRIPTION OF DEPOSITS AND ANALYZED SAMPLES

No.	Deposit	Host rock	Gangue minerals	Mineralization	Main ore minerals	Vein type*	Analyzed minerals (sample number)	References
Northern Schwarzwald								
1	Käfersteige, near Pforzheim	sandstone, granite	Fl–Brt–Qtz	Cu–Ag–Bi	Tn, Py, Gn, Sp	2	mixite group (SG168)	Meyer <i>et al.</i> (2000)
2	Neubulach	sandstone	Brt–Qtz	Cu–Ag–Bi	Bi-bearing Tn, Emp	4	mixite group (SG79Ch, SG80, SG83, SG84, SG85, SG86, SG268) calcite (SG79Ca, SG159)	Stauda <i>et al.</i> (2010b)
3	Dorothea, near Freudenstadt	sandstone, granite	Brt	Cu–Ag	Bi-bearing Tn	4	mixite group (SG97)	Kesten & Werner (2006)
Central Schwarzwald, Northern Kinzigtal fault								
4	Silberbrünne, near Gengenbach	gneiss	Qtz	Cu	Tn, Gn, Cp	2	mixite group (SG105, SG106, SG114, SG116, SG117, SG118, SG178, SG199) rhabdophane (SG118, SG200)	Stauda <i>et al.</i> (2010a)
5	Amalie, near Nordrach	gneiss	Qtz–Brt	Cu–Ag	Tn, Gn, Cp	2	mixite group (SG91, SG92, SG93, SG94, SG98, SG98mR)	Stauda <i>et al.</i> (2010a)
6	Clara, near Wolfach	gneiss	Brt–Fl–Qtz	Cu–Pb	Tn, Td, Py, Cp, Gn	2	mixite group (SG52, SG69, SG70, SG71, SG72, SG73, SG74, SG75, SG76, SG77, SG78, SG130, SG131, SG133) rhabdophane (SG54, SG57, SG58, SG59, SG61, SG62, SG63, SG64, SG65, SG180, SG181) Mn oxide (SG52)	Stauda <i>et al.</i> (2010a), Huck (1984)
7	Friedrich-Christian	gneiss	Qtz–Cal	Cu–Pb	Gn, Py, Cp	2	mixite group (SG89, SG139, SG140, SG141, SG142)	Stauda <i>et al.</i> (2010a)
8	Johann Baptist	gneiss	Qtz	Cu	Tn, Cp	2	mixite group (SG203, SG204, SG205)	Bliedtner & Martin (1986)
9	Daniel im Dehs	granite			Tn, Cp	2	mixite group (SG110, SG171, SG172)	Stauda <i>et al.</i> (2010a)
Central Schwarzwald, Wittichen								
10	Wolfgang, near Alpirsbach	granite	Brt	Co–Bi–Ag	Skt, Nc, Cp	2	mixite group (SG225)	Bliedtner & Martin (1986)
11	Rötenbach quarry, near Alpirsbach	granite	Brt	Cu–Bi	Emp, Cp, Skt, Bmt	2	mixite group (SG103, SG111)	Bliedtner & Martin (1986)
12	Schmiedestollen dump	granite	Brt	Co–Bi–Ag–U	Bi-bearing Tn, Emp, native Bi Bmt, "Pch"	2	mixite group (SG101, SG102, SG115, SG127, SG128, SG129, SG143, SG144, SG145, SG146, SG148, SG252)	Stauda <i>et al.</i> (in press)

TABLE 2 (cont'd). CLASSIFICATION AND DESCRIPTION OF DEPOSITS AND ANALYZED SAMPLES

No.	Deposit	Host rock	Gangue minerals	Mineralization	Main ore minerals	Vein type*	Analyzed minerals (sample number)	References
13	Daniel im Gallenbach	granite	Fl–Brt	Cu–Bi	Bi-bearing Tn, Emp, Gn, Wtc, Sp, Cp, native Bi	4	mixite group (SG124)	Staude <i>et al.</i> (in press)
Central Schwarzwald, Hechtsberg								
14	Hechtsberg	gneiss	Cal	Co–Bi–Cu–As	Bi-bearing Tn, Sfl, Py, Wtc	2	mixite group (SG123)	Otto (1974)
Southern Schwarzwald								
15	Amalie, near Grunern	gneiss	Qtz–Brt	Cu–Pb	Td–Tn, Gn, Cp	2	mixite group (SG224)	Staude <i>et al.</i> (2010b)
16	Knappengrund	gneiss	Fl–Qtz–Brt	Pb–Zn	Sp, Gn	2	mixite group (SG88)	Metz <i>et al.</i> (1957)
17	Teufelsgrund	gneiss	Fl–Brt	Pb–Zn	Sp–Gn	2	chukhrovite (AL31Chk) fluorite (AL31, Al31FVIII)	Metz <i>et al.</i> (1957)
18	Rotenbach–Feldberg	gneiss	carbonate	Cu	Tn–Td, Cp	§	mixite group (SG193, SG194, SG195)	
19	Lisbühl–West	gneiss	Fl–Brt–Qtz	Pb	Gn	2	mixite group (SG121, SG173)	Metz <i>et al.</i> (1957)
20	Baumhalde	gneiss	Fl–Qtz–Brt	Pb	Gn	2	rhabdophane (SG175) bastnäsite (SG53)	Metz <i>et al.</i> (1957)
21	Menzenschwand	granite	Qtz–Brt–Fl	U	Py, "Pch", Hem	¶	churchite (SG228a, SG229a, SG230a)	Hofmann (1989)
22	Gottesehre, near Urberg	gneiss	Fl–Qtz–Brt	Pb	Gn, Cp	2	mixite group (SG126)	Metz <i>et al.</i> (1957)
23	Säckingen	gneiss	Qtz	W–Cu–Bi–As	Scl, native Bi, Apy, Cc, Cp	‡	mixite group (SG201)	Werner <i>et al.</i> (1990), Schatz & Otto (1989)

§ Miocene carbonate veins; ¶ Carboniferous veins; ‡ Late magmatic phases. * Vein type after Staude *et al.* (2009). Symbols used in this listing: Apy: arsenopyrite, Bi: bismuth, Bmt: bismuthinite, Brt: barite, Cal: calcite, Cc: chalcocite, Cp: chalcopyrite, Emp: emplectite, Fl: fluorite, Gn: galena, Hem: hematite, Nc: nickeline, "Pch": "Pitchblende", Py: pyrite, Qtz: quartz, Scl: scheelite, Sfl: safflorite, Skt: skutterudite, Sp: sphalerite, Td: tetrahedrite, Tn: tennantite, Wtc: wittichenite,

magmatic fluids related to a granitic intrusion (Werner *et al.* 1990, Schatz & Otto 1989), contains some Cu ore minerals, mainly chalcocite. The U mineralization of Menzenschwand (Hofmann 1989, Hofmann & Eikenberg 1991) occurs at the only granite-hosted locality in the southern Schwarzwald investigated in the present study. Here, "pitchblende" occurs in quartz – barite – fluorite veins.

Mixite-group minerals occur in all parts of the Schwarzwald. Seventy-four samples of mixite-group minerals from 20 localities were analyzed. They usually grow as euhedral acicular or fibrous crystals in vugs or form crusts. Crystals either grow on gangue minerals (barite, fluorite or quartz) or directly on the host rock.

They reach a length of up to 5 mm and a diameter up to hundreds of μm . However, in most cases, they are only some tens or only a few μm thick and less than 1 mm long (Figs. 2a, b). Mixite-group minerals typically grow as isolated aggregates, but in rare cases, they are intergrown with other secondary minerals such as calcite (SG79Ca) or Mn oxides (SG52). The colors of mixite-group minerals vary from light to dark green to bluish green. Mixite *sensu stricto* is usually bluish green, whereas agardite is rather dark or light green. However, unambiguous distinction of end-members by color is not possible.

Like the mixite-group minerals, rhabdophane grows in vugs, but as fibrous or spherical crystals only a few

μm in diameter (Figs. 2a, b). It usually forms isolated crystals on quartz (Fig. 2c), barite or fluorite. In one case, rhabdophane crystals grow on a mixite-group mineral (SG118, Figs. 2a, b). Their colors range from white to orange. The phosphate mineral rhabdophane is not as abundant as minerals of the mixite group, and samples from only three localities from the central and southern Schwarzwald could be analyzed. Churchite, another REE phosphate, forms white fibrous crystals only on samples from the Menzenschwand U deposit, where it is relatively common. The REE hydrophosphates were identified by XRD analyses to rule out confusion with monazite and xenotime.

Bastnäsite (SG53) grows as yellowish brown needles only μm in diameter and length along cracks, and it fills fractures in quartz. It occurs at six localities in the Schwarzwald (Walenta 1992), but crystals are usually very small. Therefore, it could be isolated and analyzed from only one locality (the Baumhalde mine).

The only sample of chukhrovite analyzed (AL31Chk from the Teufelsgrund mine) shows euhedral crystals of white color, which are intergrown with a third generation of fluorite (Figs. 2e, f).

Fluorite, calcite and Mn oxides were analyzed where they are texturally and thus genetically related to REE minerals. Euhedral crystals of fluorite from Teufelsgrund (third generation of fluorite at this locality, sample AL31FIII) are intergrown with chukhrovite (AL31Chk, Fig. 2e). Both grow on an older generation of secondary fluorite (AL31F). Calcite (SG79Ca) from Neubulach is intergrown with a mixite-group mineral (SG79Ch, Fig. 2f). In addition, a calcite sinter (SG159) from Neubulach, which was precipitated from dripping water in an ancient mine and not intergrown with any other mineral, was analyzed. A Mn oxide crust (SG52; chemical composition close to asbolane and romanèchite) from the Clara mine is intergrown with a mixite-group mineral (SG52, Fig. 2g).

Water samples

Water samples were taken in Neubulach, northern Schwarzwald, in the Johann Baptist mine and the Clara mine in the central Schwarzwald, and from the Teufelsgrund mine in the southern Schwarzwald. The sample in Neubulach was taken in the Wasserstollen 530 m from the adit entrance, where maximum formation of sinter and dripping water occur. In the Teufelsgrund mine, the sample was taken ~450 m from the adit entrance, close to the blind shaft, where water was dripping from the roof. In the Johann Baptist mine, water flowing over an adit wall was sampled. Aggregates of agardite (SG205) were seen on this wall. In the Clara mine, three samples of water were taken from different levels (samples CL 2 to 4) and from a small creek (Breiet, sample CL 1) outside the mine. From drillings, it is known that the water of sample CL 2 and 4 flows along the hydro-

thermal veins, whereas sample CL 3 is draining the host rock.

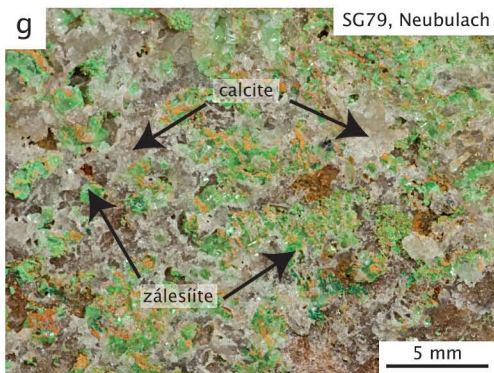
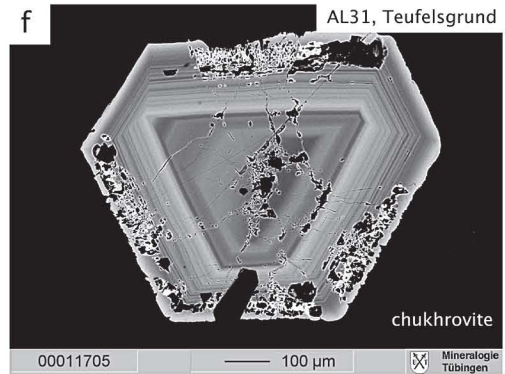
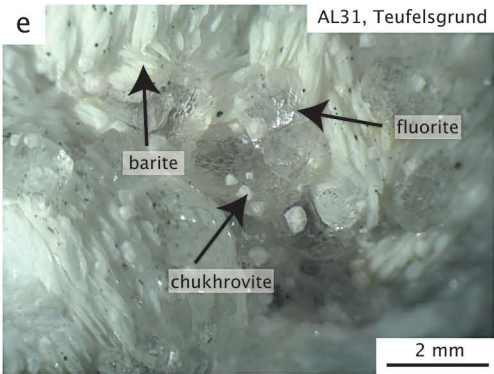
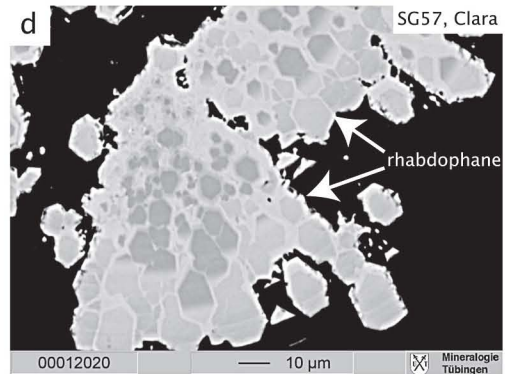
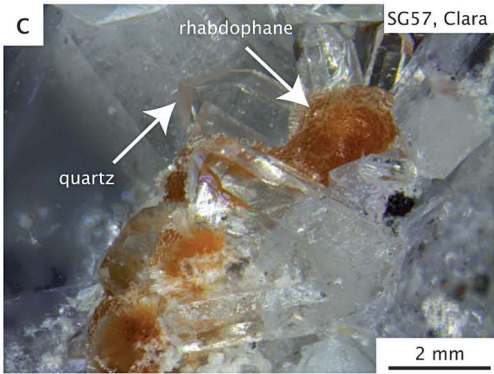
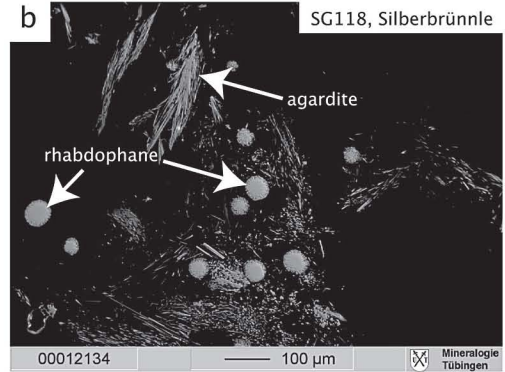
ANALYTICAL METHODS

Electron-microprobe analysis (EMPA)

Electron-microprobe analyses were performed on a JEOL JXA-8900RL Superprobe at the Fachbereich Geowissenschaften, Universität Tübingen, in wavelength-dispersive mode (WDS) at 25 kV acceleration voltage and 20 nA beam current for the mixite-group minerals. We acquired WDS scans prior to quantitative analyses so that all important elements were determined. For Al, P, Ca, Fe and Cu, we used the $K\alpha$ line, for As, Y, La, Ce, Bi, Sb and Eu, the $L\alpha$ line, for Pr, Nd, Sm, Gd and Dy, the $L\beta$ line, and for Pb the $M\beta$ line. The HREE were not sought owing to their low concentrations, below the detection limit of the microprobe. Backgrounds were chosen carefully to avoid overlaps. Peak-overlap corrections had to be applied for Eu-Pr (factor of 0.335) and As-Sb (factor of 0.00173). Further peak-overlap corrections were not necessary, as concentrations of interfering elements in the samples were not high enough to have a significant influence on the results. Counting times were 16 s on the peak and 8 s on the background position for Al, Ce, Bi, Ca and Cu, and 30 s on the peak and 15 s on the background position for all other elements. To check conditions of measurement, a synthetic crystal of mixite *sensu stricto* [$\text{BiCu}_6(\text{AsO}_4)_3\text{OH}_6 \cdot 3\text{H}_2\text{O}$; provided by Prof. Miletich-Pawliczek] was analyzed. The only elements detected were Bi, Cu and As. Detection limits of all elements are usually below 1000 ppm, only Pb has higher detection-limits, 1500 ppm. Standard deviations (2σ) are <20% for As, Cu, Ca, Ce, Nd, Sm, Eu and Gd, and <50% for all other elements.

The same analytical conditions as for mixite-group minerals were used for rhabdophane, except that a beam current of 15 nA was chosen to prevent sample destruction. Counting times were 30 s on the peak position and 15 s on the background for Y and P, and 16 s on the peak position and 8 s on the background for all other elements.

For churchite, the HREE were included in the analytical protocol. For La, Ce, Pr, Nd, Sm, Eu, Tb, Er, Yb and Y, we used the $L\alpha$ lines, for Gd, Dy and Lu, the $L\beta$ line, and for P and Ca, the $K\alpha$ line. Peak-overlap corrections were necessary for Lu-Dy (correction factor = 0.19299) and Eu-Pr (correction factor = 0.2493). Further peak-overlaps were not corrected, as standard measurements revealed only insignificant apparent concentrations of the relevant elements. Acceleration voltage was set at 20 kV. A beam current of 3 nA was chosen; test measurements had shown that the sample current was not stable at 10 or 15 nA. Detection limits are up to 1000 ppm for Ca, P, La, Ce, Pr, Nd, Tb and Yb,



and up to 1500 for Eu, Gd, Dy, Y, Er and Lu. Standard deviations (2σ) are <20% for P, Ca, Sm, Eu, Gd, Tb, Dy, Y, Er and Yb, and <50% for all other elements.

In the Mn oxides, $K\alpha$ lines were used for analysis of the sample for Mn, Co, Cu and Fe, whereas Ba was sought on the $L\alpha$ line. Acceleration voltage was 20 kV, the beam current was 20 nA.

Analytical uncertainties do not only comprise the analytical error (standard deviation) of the electron microprobe, but also effects caused by sample properties. Many of the analyzed samples are fibrous or porous, which may introduce an additional source of uncertainty compared to ideal samples, which fulfill the requirements for a high-accuracy electron-microprobe analysis. Therefore, several analyses were performed for each sample to check reproducibility and to rule out a significant influence of the above-mentioned sample properties on quality of the data.

LA-ICP-MS data

The REE concentrations in chukhrovite, bastnäsite, fluorite, calcite and the Mn oxides and two samples of agardite and rhabdophane each were determined *in situ* by laser-ablation inductively coupled plasma – mass spectrometry (LA-ICP-MS) at the Institut für Geowissenschaften, Universität Mainz, using an Agilent 7500ce quadrupole ICP-MS coupled to an ESI New Wave Research UP213 laser-ablation system with 213 nm wavelength (NWR 193 nm Excimer Laser for bastnäsite). Ablation was carried out with laser-energy densities of 2.5 J/cm² (2.77 J/cm² for bastnäsite) at 5 Hz using He as a carrier gas. The laser spot-size was 100 μ m for chukhrovite, fluorite, calcite, Mn oxides and bastnäsite, and between 40 and 100 μ m for agardite and rhabdophane. For data reduction, the software GLITTER 4.4 (Macquarie University, Sydney, Australia) was used with NIST SRM 612 as an external standard. As an internal standard, ⁴³Ca was used for chukhrovite, fluorite and calcite, ⁵⁵Mn for Mn oxides, ⁶³Cu for agardite, and ¹⁴⁰Ce for bastnäsite and rhabdophane. Concentrations were normalized to normative contents of the element used as internal standard (as is usual for

LA-ICP-MS analyses). Data for NIST SRM 612 were taken from the GeoReM database (Jochum & Nehring 2006). For details on detection limits and uncertainties, see Jacob (2006).

Water analyses

Water samples were taken in 1 L acid-cleaned PE bottles. Conductivity and pH were determined in the field; alkalinity was determined by titration. Samples were filtered through a 0.2 μ m filter using a Sartorius® filter system directly after sampling. Major anions and cations were determined by ion chromatography (Dionex ICS-1000) at the University of Tübingen, Fachbereich Geowissenschaften. Samples for REE analysis were acidified to pH 2 with 6 M HCl. For REE preconcentration after Bau & Dulski (1996), we used Sep-Pak® Classic C18 cartridges loaded with 2-ethylhexyl phosphate. Samples were passed through the cartridges with a flow rate of 12 mL/min. To remove matrix elements, the cartridges were washed with 10 mL 0.01 M HCl at a flow rate of 3 mL/min. The REE were concentrated in solution by elution with 40 mL 6 M HCl at a flow rate of 3 mL/min. By evaporation, this solution was reduced to incipient dryness and taken up with 0.5 M HNO₃. Throughout the whole concentration process, only Suprapur® reagents were used. Preconcentration of the REE was done at the University of Tübingen, Fachbereich Geowissenschaften, and the ICP-MS analyses were carried out at the Ocean Lab, Jacobs University Bremen. For detailed information about analyses and interferences, see Alexander (2008).

Prior to preconcentration, a Tm spike was added to the sample. By analyzing concentrated and unconcentrated aliquots of a sample, yields for REE preconcentration can be determined. The total error of REE determination was estimated to be better than 15%, based on repeated analyses of standard solutions.

RESULTS: REE MINERALS

Arsenates: mixite-group minerals [REE,Bi,Ca,Pb]
 $Cu_6[AsO_4,AsO_3OH]_3OH_6 \cdot 3H_2O$

Our EMPA results for mixite-group minerals were normalized to ten cations (for representative results, see Table 3; the full range of analytical results is provided in the electronic supplement, available from the Depository of Unpublished Data on the MAC website [document Schwarzwald CM49_1305]). Ionic charges were balanced by substituting AsO_3OH^{2-} for AsO_4^{3-} if the ionic balance was negative, or O^{2-} for OH^- if the ionic balance was positive. The H₂O content was calculated by the difference between the analyzed total and 100 wt%.

Most analyzed mixite-group samples contain either Bi and Ca or REE and Ca in varying proportions at the

FIG. 2. Selected examples of the samples investigated in the present study. Mixite-group mineral and rhabdophane from Silberbrünnle (SG118) (a) and back-scattered electron (BSE) image (b). Rhabdophane (SG57) from Clara (c) and back-scattered electron image (d). Barite, fluorite and chukhrovite (AL31) from Teufelsgrund (e) and BSE image (f). Intergrown calcite and mixite-group mineral (SG79) from Neubulach (g). Intergrown mixite-group mineral and Mn oxides (SG52) from the Clara mine (h). Differences of brightness in BSE images are caused by varying proportions of HREE, LREE, Y and Ca.

M1 site (Fig. 3). Both types can have Pb fractions of up to 0.4 out of one atom per formula unit (*apfu*), but Ca–REE–Pb compositions are more common than Ca–Bi–Pb compositions. However, Bi–REE–Ca compositions only occur where Ca contents are high (above 0.5 *apfu*). Bismuth concentrations in these samples reach up to 0.29 *apfu*. Pure Bi–REE compositions were not observed.

The M2 site is clearly Cu-dominant, and Al contents are rather low and usually below 0.5 out of 6 *apfu*. Iron contents are even lower, and only single analyses reach up to 0.5 *apfu*, whereas most samples are Fe-poor, with up to 0.1 *apfu*.

At the X site, As is the dominant element in all samples. Antimony is negligible, usually below 0.01 *apfu*, and it never reaches more than 0.1 *apfu*. In contrast, P reaches up to 1.1 out of 3 *apfu*.

TABLE 3. SELECTED EMPA DATA FOR MIXITE-GROUP MINERALS

Locality	Neubulach	Clara	Schmiede- stollen dump	Gottesehre Urberg	Amalie Grunern
Sample no.	SG79C_1	SG52_1	SG143_1	SG126_2	SG224_2
CaO wt%	3.48	2.41	0.76	0.94	1.38
PbO			b.d.l.	8.18	5.58
Bi ₂ O ₃	4.13	b.d.l.	18.58	b.d.l.	b.d.l.
La ₂ O ₃	0.22	3.21	b.d.l.	1.40	2.37
Ce ₂ O ₃	1.07	0.65	b.d.l.	1.40	4.47
Pr ₂ O ₃	0.17	0.70	b.d.l.	0.26	0.43
Nd ₂ O ₃	1.02	2.78	b.d.l.	1.19	1.34
Sm ₂ O ₃	0.44	0.62	b.d.l.	0.34	b.d.l.
Eu ₂ O ₃	0.26	0.40	b.d.l.	0.11	0.09
Gd ₂ O ₃	0.50	0.45	b.d.l.	0.44	b.d.l.
Dy ₂ O ₃	0.14	0.07	b.d.l.	0.14	b.d.l.
Y ₂ O ₃	0.65	0.58	b.d.l.	1.68	b.d.l.
CuO	42.35	42.05	42.48	41.21	45.51
FeO	0.79	0.24	b.d.l.	0.05	b.d.l.
Al ₂ O ₃	0.27	2.70	0.05	b.d.l.	0.05
As ₂ O ₅	31.41	31.01	26.29	24.81	28.92
P ₂ O ₅	0.15	0.39	0.22	2.11	0.17
Sb ₂ O ₅	b.d.l.	b.d.l.	0.06	b.d.l.	b.d.l.
Σ	87.04	88.30	88.61	84.26	90.51
dominant cation at M1 site					
	Ca	La	Bi	Y	Ce
REE <i>apfu</i>	0.30	0.61	0.00	0.52	0.55
Ca	0.67	0.45	0.15	0.19	0.25
Bi	0.19	0.00	0.89	0.00	0.00
Pb			0.00	0.41	0.26
Σ M1 site	1.16	1.05	1.04	1.11	1.06
dominant cation at M2 site					
	Cu	La	Bi	Y	Ce
Cu	5.72	5.50	5.95	5.76	5.90
Fe	0.11	0.03	0.00	0.01	0.00
Al	0.06	0.55	0.01	0.00	0.01
Σ M2 site	5.88	6.08	5.96	5.77	5.91
dominant cation at X site					
	As	La	Bi	Y	Ce
As	2.94	2.81	2.96	2.79	3.01
P	0.02	0.06	0.03	0.33	0.02
Sb	0.00	0.00	0.00	0.00	0.00
Σ X site	2.96	2.86	3.00	3.12	3.04

b.d.l.: below detection limit; Σ cations is set at 10 *apfu*.

For the REE-dominant end-members (agardite), the nomenclature of Levinson (1966) was applied. Accordingly, agardite-(Ce) is most common, but there are also agardite-(La), agardite-(Nd) and agardite-(Y) from the NKf and from the southern Schwarzwald (Fig. 4).

Only LREE from La to Gd, in addition to Dy and Y, were present in concentrations high enough to be detected by electron microprobe; all other REE were found to be below the detection limit. The LA–ICP–MS data for two samples from the Clara mine (Fig. 5) show that HREE are depleted with respect to LREE if normalized to Post-Archean Australian Shale (PAAS, Taylor & McLennan 1985). Comparison of LREE data from EMPA and LA–ICP–MS shows good agreement between the two methods (Fig. 5). Relative differences between the results from EMPA and LA–ICP–MS can be explained by the specific ablation behavior of a mineral, as LA–ICP–MS data are calibrated to an external glass standard (NIST SRM 612), which has different ablation properties. Furthermore, analyses made with the two methods are performed on different volumes of sample, which can have an influence on exact compositions. Taking these considerations and the above-mentioned analytical difficulties for EMPA into account, results obtained by the two methods are in good agreement. The only exception is La, for which consistently higher concentrations were determined with LA–ICP–MS compared to EMPA. The reason for this discrepancy is unclear.

Cerium and Eu anomalies were calculated using the formula $Ce/Ce^* = Ce_{norm}/(La_{norm} \cdot Pr_{norm})^{0.5}$ and $Eu/Eu^* = Eu_{norm}/(Sm_{norm} \cdot Gd_{norm})^{0.5}$, respectively. The Eu anomaly is invariably positive, the Ce anomaly is either nonexistent, slightly positive or, in only a few cases, negative (e.g., SG52; Fig. 6).

Phosphates: rhabdophane REEPO₄•H₂O and churchite REEPO₄•2H₂O

Rhabdophane samples from the Clara mine (central Schwarzwald/NKF, 12 samples), Silberbrünnle (central Schwarzwald/NKF, two samples) and Baumhalde (southern Schwarzwald, one sample) were analyzed. Molar concentrations were normalized to 1 *apfu* phosphorus (for representative results, see Table 4). Totals vary between 84 and 102%. As rhabdophane contains 7 wt% zeolitic water (Hikichi *et al.* 1996, Assaouadi *et al.* 2000), totals should be ~93%. Lower totals can occur if the samples are highly porous, higher totals can be due to the loss of zeolitic water prior to or during analysis (Hikichi *et al.* 1996). Most rhabdophane samples are Ce-dominant; one sample (SG118, Silberbrünnle) even reaches a Ce content of up to 0.76 *apfu*. One sample from the Silberbrünnle mine is clearly Nd-dominant (SG200, up to 0.35 *apfu* Nd), two samples (SG64 and SG180, Clara mine) are La-dominant (0.19 to 0.26 *apfu* La). All other REE are present in minor concentrations; the HREE (Tb and from Ho to Lu) were not detectable

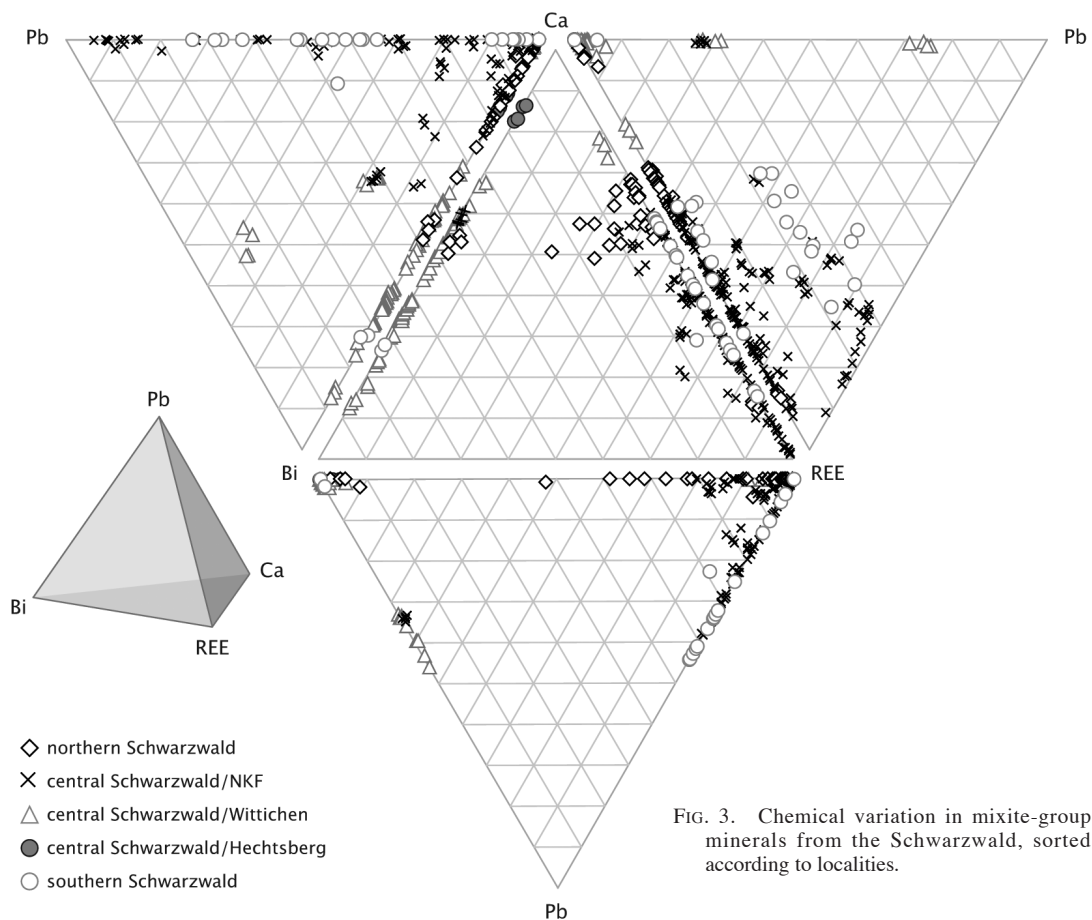


FIG. 3. Chemical variation in mixite-group minerals from the Schwarzwald, sorted according to localities.

by EMPA. All samples contain minor amounts of Ca (0.02 to 0.1 *apfu*). Lead is only a minor element in most samples (from 0 to 0.1 *apfu*), but some samples have elevated Pb contents of 0.04 (SG64) and 0.07 (SG118) *apfu*, and the samples SG54, SG180 and SG181 even contain 0.27 to 0.31 *apfu* Pb. A sample from Silberbrünnle (SG118) is not only very Ce-rich, but it is also the only sample that contains elevated amounts of As (up to 0.1 *apfu*) and Cu (0.06 to 0.08 *apfu*).

Normalized to PAAS, all samples have a positive Eu anomaly (Fig. 7). They range from $\text{Eu}/\text{Eu}^* = 2.54$ to 3.89 for most samples. Only samples SG175 from Baumhalde and SG200 from Silberbrünnle have a smaller Eu anomaly, 1.92 to 2.11. Most samples do not show a Ce anomaly; only sample SG118 (Silberbrünnle) has a positive Ce anomaly ($\text{Ce}/\text{Ce}^* = 13.1$ to 21.6). The sample with the strongest negative Ce anomaly is also from Silberbrünnle (SG200; $\text{Ce}/\text{Ce}^* = 0.03$ to 0.04). A few other samples from the Clara mine have a less pronounced negative Ce anomaly (Ce/Ce^* in the range 0.45 to 0.86).

In the three samples of churchite from Menzenschwand, Ca, P, and all REE except Ho and Tm could be detected by EMPA. Molar concentrations were normalized to 1 *apfu* phosphorus (for representative results, see Table 5). Totals vary between 80 and 93%. All samples are clearly Y-dominant, with Y contents between 0.6 and 0.7 *apfu*. Sums of all other REE are between 0.22 and 0.30 *apfu*. Calcium varies from 0.02 to 0.08 *apfu*. Normalized to PAAS, all samples are relatively depleted in LREE (Fig. 7). Cerium anomalies were determined where possible. They are nonexistent to strongly negative ($\text{Ce}/\text{Ce}^* = 0.03$ to 1.01). The Eu anomaly ranges from slightly negative (0.72) to slightly positive (1.21).

Carbonates: *bastnäsite REECO₃F*

The REE concentrations in bastnäsite (SG53) from Baumhalde are normalized to one formula unit, assuming F and CO₂ concentrations to be stoichiometrically ideal (Table 6). Cerium, the dominant REE, reaches 27.22 wt%. Normalized to PAAS, bastnäsite is

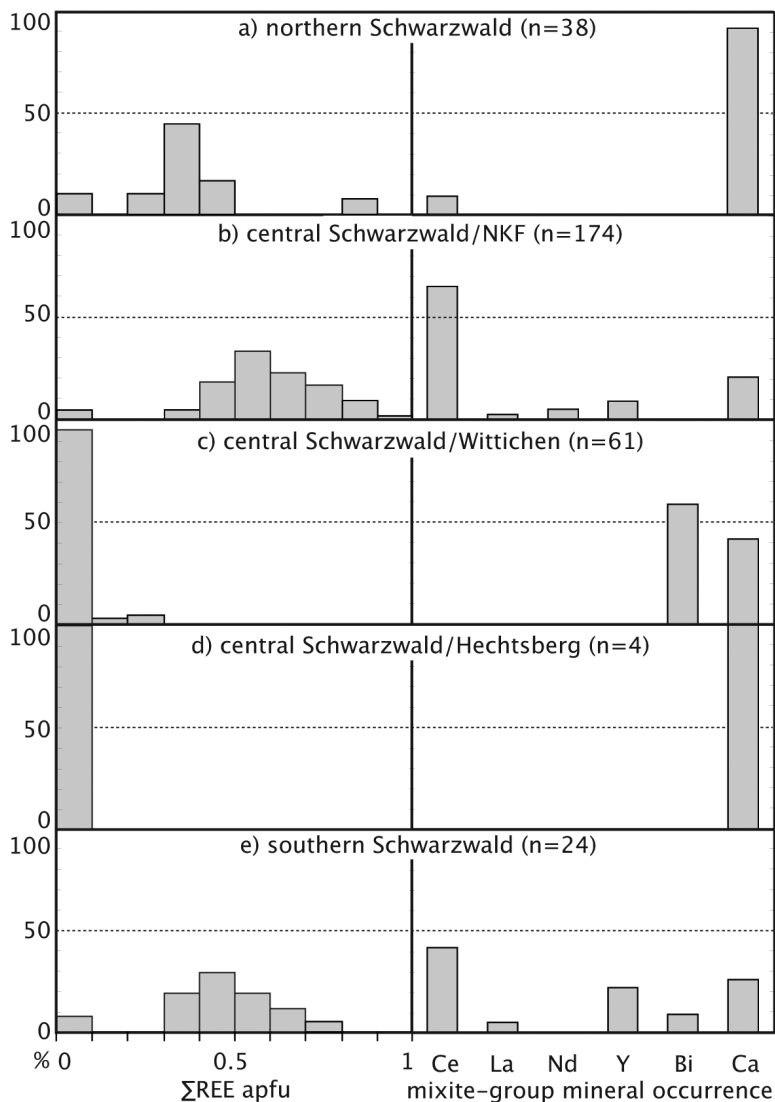


FIG. 4. Occurrence of mixite-group mineral end-members and their REE contents in the Schwarzwald, sorted by localities.

enriched in LREE compared to HREE. Europium shows a positive anomaly (1.51 to 1.56, Fig. 7), and the Y:Ho ratio is 31.1 and 32.5.

Fluoride: chukhrovite $Ca_3REEAl_2SO_4F_{13} \cdot 10H_2O$

The analyzed chukhrovite (AL31Chk) from the Teufelsgrund mine contains 12.7 to 14.8 wt% Σ REE (normalized to 20 wt% Ca, Table 7). The crystal is chemically zoned (Figs. 2f, 8a). Neodymium is the

dominant REE in the inner part of the crystal [2.6 wt%, 0.23–0.24 apfu, chukhrovite-(Nd)], whereas Ce is dominant in its outer part [3.3 to 3.4 wt%, 0.27–0.33 apfu, chukhrovite-(Ce)]. Normalized to PAAS, the LREE and HREE are depleted relatively to the middle REE (MREE). There is no Ce anomaly, but a positive Eu anomaly (1.99 to 2.18) present in all zones of the crystal. The Y:Ho ratio is between 11.1 and 24.0.

TABLE 4. SELECTED EMPA DATA ON RHABDOPHANE

Locality Sample no.	Clara Silberbrünne		Clara Silberbrünne		
	SG62_1	SG118_4	SG62_1	SG118_4	
CaO wt%	1.61	1.48	Nd ₂ O ₃ wt%	10.30	1.57
PbO	b.d.l.	6.89	Sm ₂ O ₃	2.52	b.d.l.
FeO	n.a.	0.18	Eu ₂ O ₃	1.50	b.d.l.
CuO	n.a.	2.29	Gd ₂ O ₃	1.94	b.d.l.
Bi ₂ O ₃	n.a.	0.04	Dy ₂ O ₃	0.45	b.d.l.
Al ₂ O ₃	0.43	b.d.l.	Y ₂ O ₃	2.09	0.17
La ₂ O ₃	12.72	2.24	P ₂ O ₅	31.73	27.18
Ce ₂ O ₃	25.52	54.35	As ₂ O ₅	n.a.	4.99
Pr ₂ O ₃	2.74	0.15	Sb ₂ O ₅	n.a.	b.d.l.
			Σ	93.67	101.67
Ca apfu	0.06	0.06	Nd apfu	0.14	0.02
Pb	0.00	0.07	Sm	0.03	0.00
Fe		0.01	Eu	0.02	0.00
Cu		0.07	Gd	0.02	0.00
Al	0.02	0.00	Dy	0.01	0.00
Bi		0.00	Y	0.04	0.00
La	0.17	0.03	Σ A site	0.90	1.05
Ce	0.35	0.78	P	1.00	0.90
Pr	0.04	0.00	As		0.10
			Sb		0.00
			Σ B site	1.00	1.00

TABLE 5. SELECTED EMPA DATA ON CHURCHITE

Locality Sample	Menzenschwand		Menzenschwand		
	SG228a_10	SG229a_3	SG228a_10	SG229a_3	
CaO wt%	0.44	0.54	Gd ₂ O ₃ wt%	3.32	3.66
Y ₂ O ₃	34.12	32.17	Dy ₂ O ₃	3.28	5.24
La ₂ O ₃	0.57	0.08	Tb ₂ O ₃	0.54	0.69
Ce ₂ O ₃	0.22	0.60	Er ₂ O ₃	1.56	2.30
Pr ₂ O ₃	1.02	0.23	Yb ₂ O ₃	1.16	1.90
Nd ₂ O ₃	4.69	1.98	Lu ₂ O ₃	0.32	0.39
Sm ₂ O ₃	1.87	2.06	P ₂ O ₅	31.28	31.90
Eu ₂ O ₃	0.50	0.66	Σ	84.87	84.41
Ca apfu	0.02	0.02	Gd apfu	0.04	0.04
Y	0.69	0.63	Dy	0.04	0.06
La	0.01	0.00	Tb	0.01	0.01
Ce	0.00	0.01	Er	0.02	0.03
Pr	0.01	0.00	Yb	0.01	0.02
Nd	0.06	0.03	Lu	0.00	0.00
Sm	0.02	0.03	Σ	0.95	0.90
Eu	0.01	0.01			

The compositions are recalculated on the basis of 1.00 atoms of P per formula unit.

n.a.: not analyzed, b.d.l.: below detection limit. Compositions are normalized to Σ B = 1 atom per formula unit.

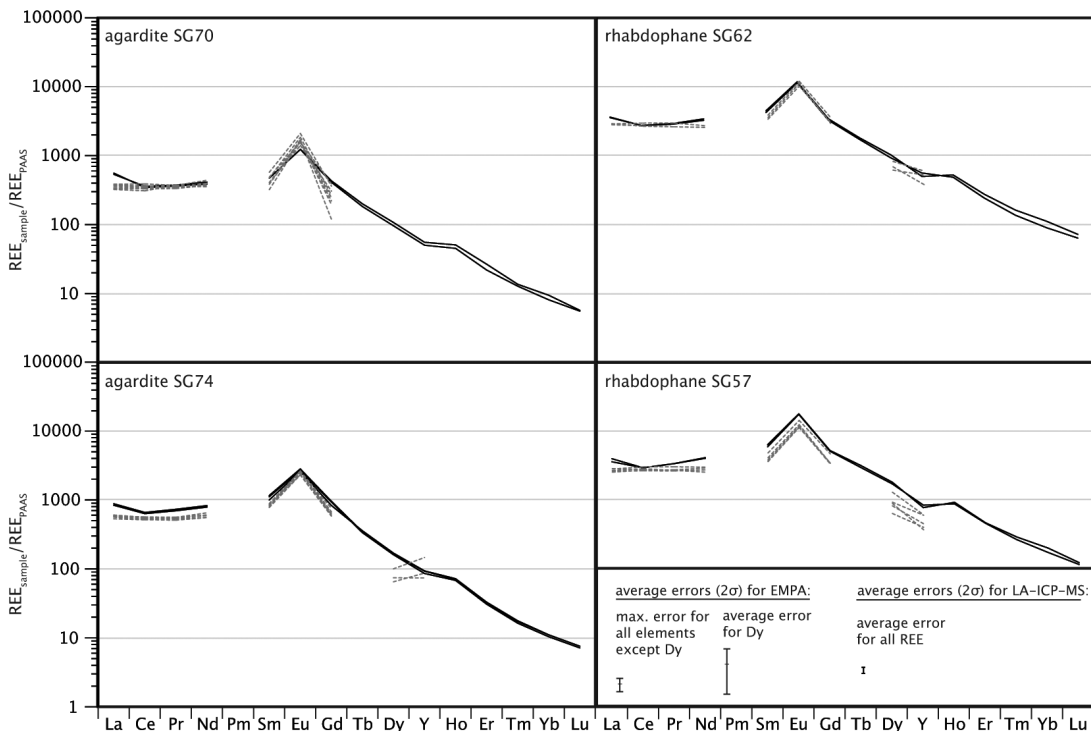


FIG. 5. REE patterns in mixite-group minerals and rhabdophane analyzed with EMPA (grey dashed line) and LA-ICP-MS (black line).

RESULTS: COGENETIC SECONDARY MINERALS

Fluorite

Secondary fluorite (AL31FI) from Teufelsgrund contains REE in the low ppm range ($\Sigma\text{REE} = 80 - 140$ ppm; Table 7). In some cases, the LREE are slightly depleted compared to PAAS (Fig. 8a). No Ce anomaly is developed, the Eu anomaly is positive (2.35 to 2.97), and the Y:Ho ratio ranges from 23.0 to 40.8.

A third generation of fluorite (AL31FIII) overgrows the secondary fluorite AL31FI and is intergrown with chukhrovite (AL31Chk). Its REE content is in the same range as that of the secondary fluorite, but it is more strongly depleted in LREE than sample AL31FI and displays a positive Eu anomaly (Eu/Eu* between 1.74

and 2.91). The Y:Ho ratio is between 33.48 and 97.60. A Ce anomaly is not present.

These results from Teufelsgrund compare well with data of Loges *et al.* (2009), who analyzed primary and secondary (\pm recent) fluorite from the Clara mine near Wolfach by LA-ICP-MS for their REE contents. They found that primary fluorite is relatively depleted in LREE without a Ce anomaly, whereas secondary fluorite is usually less depleted in LREE compared to HREE and displays a negative Ce anomaly.

Calcite

The calcite sinter (SG159) from Neubulach contains REE in the ppb range (Table 8). It is relatively depleted in LREE and displays a negative Ce anomaly (Ce/Ce* = 0.07, Fig. 8b). No pronounced Eu anomaly is present (Eu/Eu* = 1.58). The calcite (SG79Ca) that is intergrown with a mixite-group mineral shows similar characteristics (Eu/Eu* = 1.36), but with a less pronounced Ce anomaly (Ce/Ce* = 0.39). The Y:Ho ratio in both samples of calcite is similar (42.71 and 32.02 for SG159 and SG79Ca, respectively).

Mn oxides

The Mn crust (SG52) consists of Mn oxides of variable composition. Most of the sample is a Cu-Co-rich Mn oxide (44.06 to 45.24 wt% MnO₂, 16.65 to 18.19 wt% CoO, 17.81 to 20.44 wt% CuO, <0.4 wt% BaO; Table 9), whereas some parts are Ba-rich (68.3 wt% Mn₂O₃, 5.47 wt% CoO, 8.90 wt% CuO, 11.94 wt% BaO). These compositions are similar to asbolane [(Cu,Co,Ni)_{2-x}Mn(O,OH)₄•xH₂O] and romanèchite [(Ba,H₂O)₂Mn₅O₁₀]. Normalized to 1 and 5 *apfu* Mn, respectively, sums of other cations are between 1.08 and

TABLE 6. LA-ICP-MS DATA ON BASTNÄSITE

	SG53_1	SG53_2	SG53_3	SG53_4	SG53_5
La wt%	15.4	15.1	14.8	16.2	15.7
Ce	31.9	32.3	32.7	29.8	31.1
Pr	2.73	2.64	2.72	2.84	2.73
Nd	11.4	11.3	11.3	11.9	11.6
Sm	2.38	2.35	2.34	2.49	2.43
Eu	0.655	0.626	0.623	0.671	0.654
Gd	1.65	1.62	1.61	1.71	1.69
Tb	0.158	0.156	0.156	0.167	0.162
Dy	0.617	0.605	0.613	0.647	0.639
Y	2.93	3.02	2.99	3.23	3.10
Ho	0.084	0.084	0.087	0.094	0.087
Er	0.153	0.153	0.156	0.164	0.159
Tm	0.015	0.015	0.015	0.016	0.015
Yb	0.067	0.068	0.069	0.073	0.068
Lu	0.007	0.008	0.007	0.008	0.008

The results are normalized to ΣREE equal to one atom per formula unit.

TABLE 7. LA-ICP-MS DATA ON FLUORITE AND CHUKHROVITE

	AL31 FI-1	AL31 FI-2	AL31 FI-3	AL31 FI-4	AL31 FI-5	AL31 FI III-1	AL31 FI III-2	AL31 FI III-3	AL31 FI III-4	AL31 Chk-1	AL31 Chk-2	AL31 Chk-3	AL31 Chk-4
La ppm	22.1	4.16	8.10	8.10	9.14	4.41	4.19	1.62	5.67	8495	7880	11570	17597
Ce	45.3	10.1	16.4	16.3	17.0	8.15	7.40	3.16	13.8	26165	24718	32616	42454
Pr	5.54	1.50	2.19	2.27	2.30	1.15	1.02	0.449	2.00	4780	4648	5431	6073
Nd	21.0	6.72	9.38	9.47	9.71	5.19	4.59	2.31	9.09	26523	25872	28463	28143
Sm	4.43	1.85	2.96	2.88	3.72	2.31	1.99	0.934	2.26	8459	8180	8472	7288
Eu	2.41	1.02	1.83	1.88	2.68	1.89	1.57	0.783	0.901	3917	3758	3735	3083
Gd	3.27	2.24	3.77	3.87	6.00	4.56	3.71	1.71	2.61	9930	9649	8793	6057
Tb	0.49	0.48	0.803	0.87	1.32	1.11	0.898	0.407	0.568	1380	1323	1149	675
Dy	3.40	3.87	6.63	7.03	10.4	9.21	7.93	3.55	5.55	6982	6575	5528	3014
Y	17.5	40.1	51.7	47.9	55.5	78.1	70.9	30.9	174	12090	11712	12340	10213
Ho	0.666	0.885	1.47	1.50	2.18	2.10	1.80	0.798	1.61	978	917	752	384
Er	1.98	2.87	4.55	4.59	6.43	6.51	5.49	2.57	5.93	1725	1601	1314	660
Tm	0.305	0.477	0.734	0.726	1.00	0.995	0.930	0.394	1.02	150	137	114	52
Yb	2.50	3.38	5.93	5.75	7.52	7.77	7.45	3.24	8.04	673	612	523	259
La	0.343	0.474	0.809	0.828	1.07	1.07	1.04	0.484	1.15	58	52	45	26

Symbols: FI: fluorite, Chk: chukhrovite.

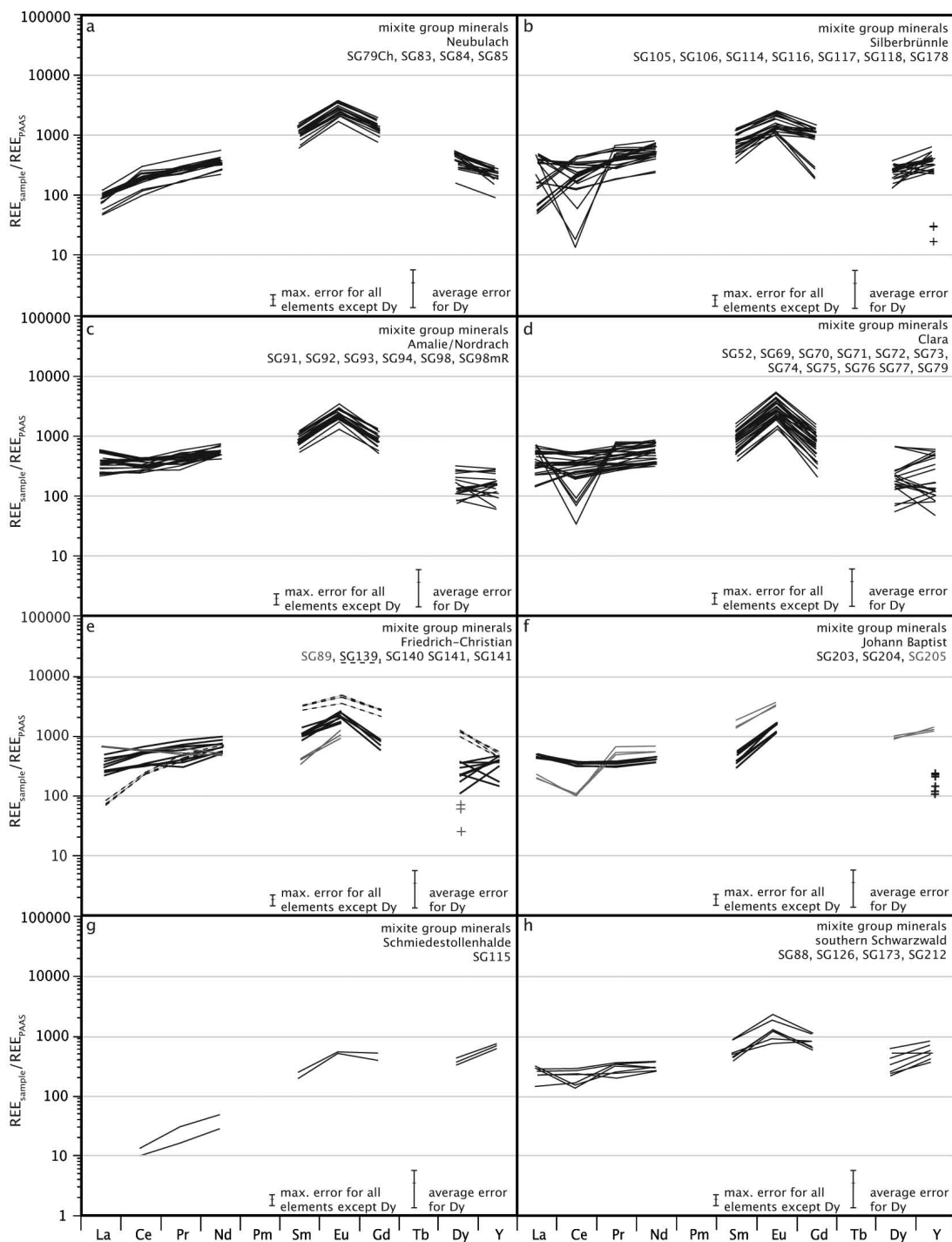


FIG. 6. Representative REE patterns of mixite-group minerals (determined by EMPA).

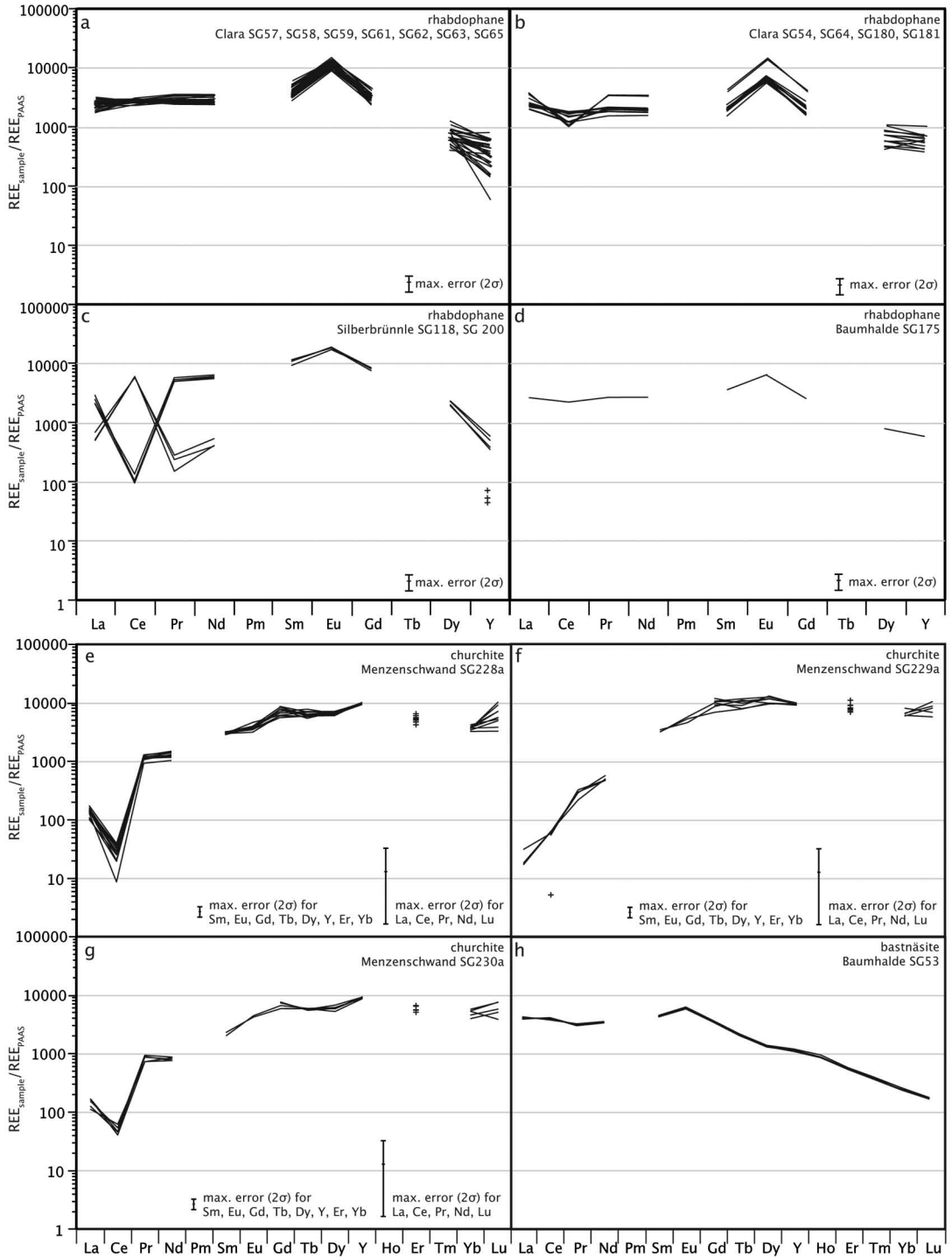


FIG. 7. Representative REE patterns of rhabdophane and churchite (determined by EMPA) and bastnäsite (determined by LA-ICP-MS).

0.98 for the Cu–Co-rich compositions and 1.89 for the Ba-rich composition.

The REE concentrations in the Co–Cu-rich Mn oxide are between 350 and 500 ppm (Σ REE), Ba-rich Mn oxide reaches REE concentrations of 1800 ppm. Normalized to PAAS (Fig. 8c), the Ba-rich Mn oxide is enriched in LREE and displays a positive Eu anomaly ($\text{Eu}/\text{Eu}^* = 3.2$), whereas the positive Ce anomaly is only weakly developed ($\text{Ce}/\text{Ce}^* = 1.2$). The HREE are relatively depleted. The Cu–Co-rich Mn oxide shows a similar Eu anomaly ($\text{Eu}/\text{Eu}^* = 3.2$), but its Ce anomaly is significantly stronger (Ce/Ce^* in the range 4.9 to 27.2).

RESULTS: WATER SAMPLES

The water from the Wasserstollen of the Hella Glück mine in Neubulach is a hydrogen carbonate water with a pH of 8.5 (Table 10). It contains REE in the ppt range (Σ REE = 100 ppt). Normalized to PAAS, the LREE are depleted compared to the HREE, with a negative Ce anomaly ($\text{Ce}/\text{Ce}^* = 0.1$), but no distinctive Eu anomaly ($\text{Eu}/\text{Eu}^* = 1.4$) is present (Fig. 9a).

The water sample from the Teufelsgrund mine has a pH of 6.6 and is sulfate-dominant, with a total REE content of 650 ppt (Table 10). Normalized to PAAS, no strong depletion of HREE or LREE is observed. A positive Eu anomaly ($\text{Eu}/\text{Eu}^* = 1.94$) and a negative Ce anomaly ($\text{Ce}/\text{Ce}^* = 0.21$) are present (Fig. 9b).

The Johann Baptist mine water is hydrogen-carbonate-dominated with a pH of 6.7 (Table 10). The sum of REE is 80 ppt, normalized to PAAS; the LREE are slightly depleted, and a negative Ce anomaly ($\text{Ce}/\text{Ce}^* = 0.18$) and a positive Eu anomaly ($\text{Eu}/\text{Eu}^* = 2.5$) are present (Fig. 9c).

The water samples that percolated along the veins of the Clara mine have pH values of 6.6 and 6.7 (Table 10), are relatively depleted in LREE, and show no pronounced Ce anomaly (CL2 $\text{Ce}/\text{Ce}^* = 0.70$ and CL4 $\text{Ce}/\text{Ce}^* = 0.45$). Total REE contents are 40 and 60 ppt. The samples from the host rock and the stream have pH values of 6.5 and 7.3, are less depleted in LREE,

and display a negative to strongly negative Ce anomaly (CL1 $\text{Ce}/\text{Ce}^* = 0.58$ and CL3 $\text{Ce}/\text{Ce}^* = 0.02$; Fig. 9d). The sums of REE are 200 and 120 ppt.

DISCUSSION

Mixite-group compositions

Our EMPA results on seventy-four mixite-group minerals imply that there is a miscibility gap between agardite and mixite, whereas the miscibility of agardite with zálesite and of mixite with zálesite is complete (Fig. 3). Although it seems that miscibility between agardite and mixite does not exist, zálesite with an elevated amount of both REE and Bi is present. As there are no data on true plumboagardite, no information about the miscibility with other end-members can be given. However, elevated amounts of Pb can be observed in agardite as well as mixite, suggesting a complete miscibility of Pb in agardite and mixite. A

TABLE 9. LA-ICP-MS DATA ON Mn OXIDE

	SG52Mn-1	SG52Mn-2	SG52Mn-3		SG52Mn-4
MnO ₂ wt%	44.06	45.24	44.35	Mn ₂ O ₃ wt%	68.30
CaO	0.13	0.14	0.17	CaO	0.08
Fe ₂ O ₃	0.14	1.06	0.85	Fe ₂ O ₃	0.14
CoO	18.19	18.12	16.65	CoO	5.47
NiO	2.32	2.08	2.27	NiO	0.99
CuO	20.44	19.25	17.81	CuO	8.90
ZnO	0.92	0.88	1.12	ZnO	0.61
As ₂ O ₅	0.03	0.07	0.09	As ₂ O ₅	0.42
BaO	0.10	0.41	0.07	BaO	11.94
PbO	0.06	0.15	0.06	PbO	2.08
Σ	85.38	86.30	82.17		95.83
Ca <i>apfu</i> *	0.00	0.00	0.01	Ca <i>apfu</i> **	0.01
Fe	0.00	0.01	0.01	Fe	0.01
Co	0.48	0.46	0.44	Co	0.46
Ni	0.06	0.05	0.06	Ni	0.08
Cu	0.51	0.47	0.44	Cu	0.71
Zn	0.02	0.02	0.03	Zn	0.05
As	0.00	0.00	0.00	As	0.01
Ba	0.00	0.01	0.00	Ba	0.50
Pb	0.00	0.00	0.00	Pb	0.06
Σ	1.08	1.03	0.98		1.89
La ppm	6.99	35.67	12.16	La ppm	413.73
Ce	450.08	328.39	293.23	Ce	833.12
Pr	2.09	6.81	3.28	Pr	66.24
Nd	10.63	31.10	15.64	Nd	275.68
Sm	4.00	8.64	5.40	Sm	66.08
Eu	2.59	5.48	3.35	Eu	37.06
Gd	3.69	7.53	4.62	Gd	46.08
Tb	0.60	1.08	0.72	Tb	5.49
Dy	2.55	4.36	2.96	Dy	21.93
Y	8.70	12.60	8.80	Y	51.22
Ho	0.41	0.65	0.43	Ho	2.66
Er	0.84	1.20	0.86	Er	5.10
Tm	0.13	0.17	0.11	Tm	0.56
Yb	0.87	1.16	0.71	Yb	4.07
Lu	0.12	0.13	0.08	Lu	0.53

* Amounts are normalized to one Mn atom per formula unit, as monitored by electron-microprobe analysis. ** The amount is normalized to five Mn atoms per formula unit, as monitored by electron-microprobe analysis.

TABLE 8. LA-ICP-MS DATA ON CALCITE

	SG79-4	SG159-4	SG79-4	SG159-4
CaO wt%	56.74	55.01	Tb	0.085
La ppm	0.185	0.054	Dy	0.644
Ce	0.205	0.015	Y	5.59
Pr	0.076	0.048	Ho	0.175
Nd	0.418	0.349	Er	0.640
Sm	0.459	0.155	Tm	0.119
Eu	0.124	0.085	Yb	1.10
Gd	0.396	0.405	Lu	0.186
				0.044

These data are normalized to the amount of CaO measured by electron-microprobe analysis.

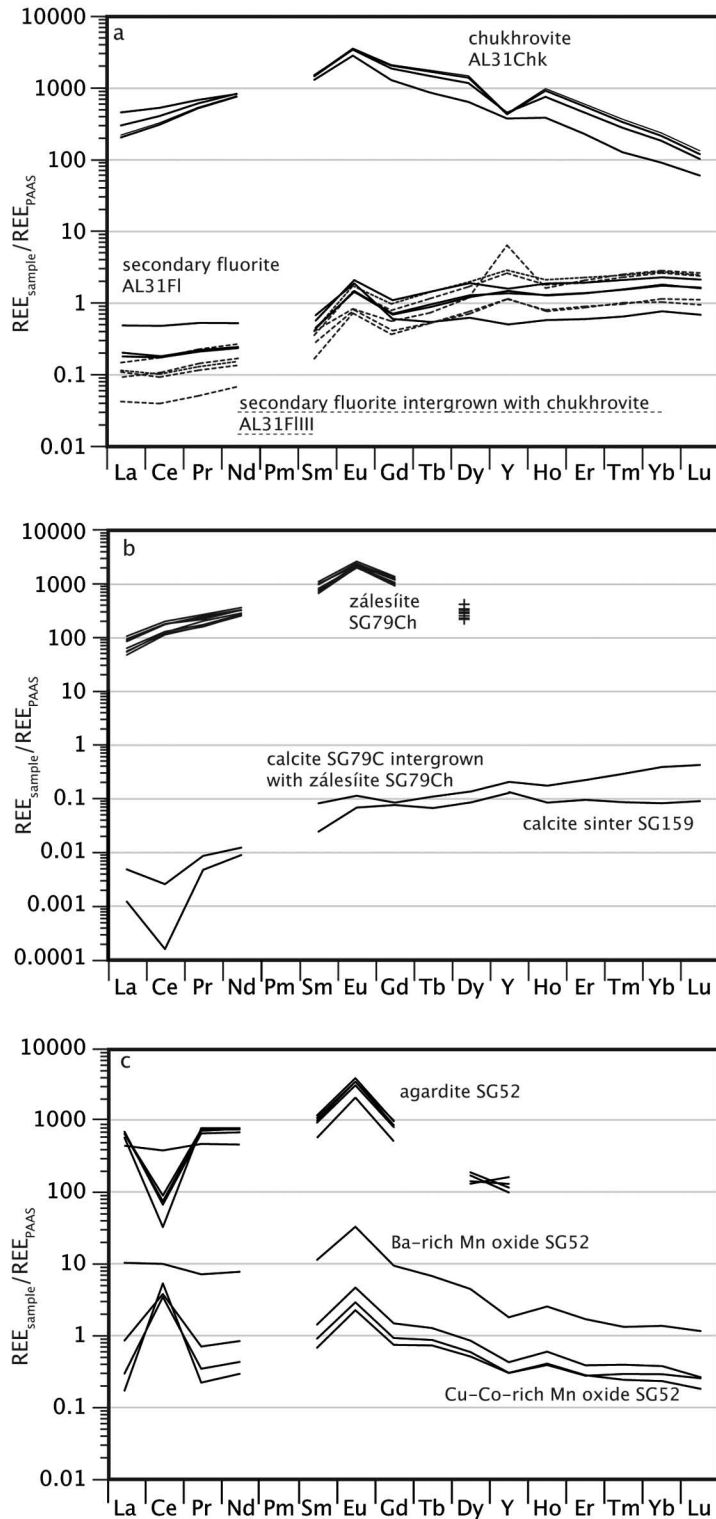


FIG. 8. REE patterns of cogenetic chukhrovite and fluorite (a), zálesítite and calcite (b) and zálesítite and Mn oxides (c). All REE determined by LA-ICP-MS, except for zálesítite and agardite (EMPA).

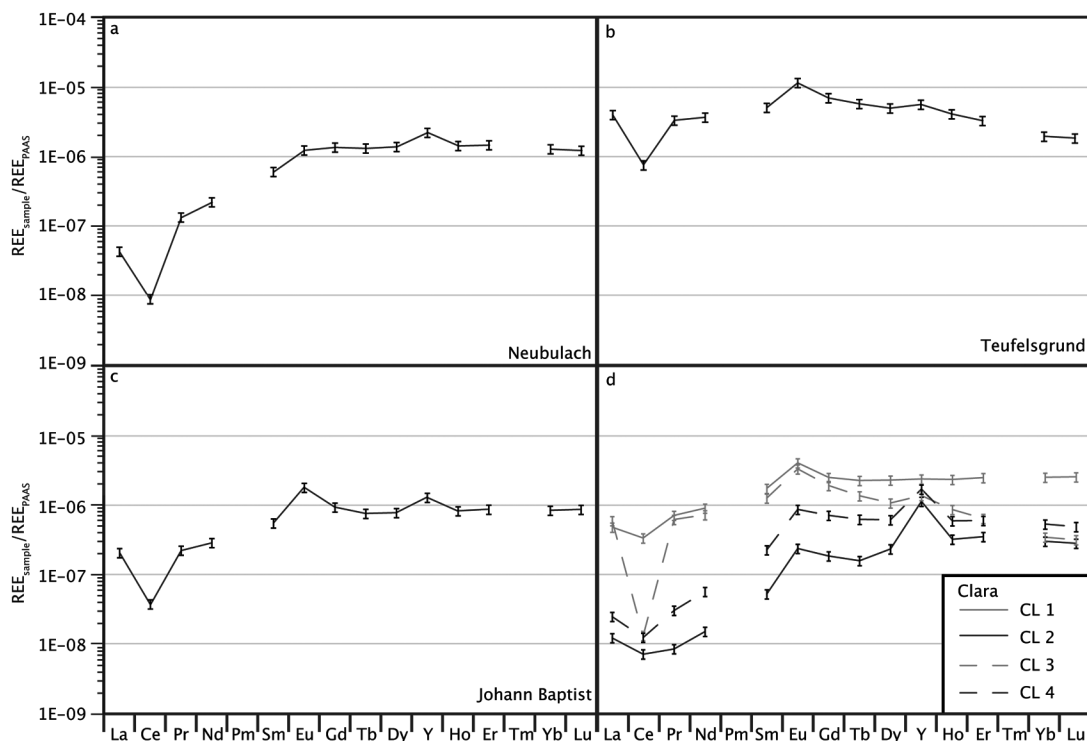


FIG. 9. REE pattern for water samples normalized with respect to PAAS from a) Neubulach, b) Teufelsgrund, c) Johann Baptist and d) the Clara mine: CL 1 (grey line): water from creek outside the mine, CL2 (black line): water from quartz–fluorite vein; CL3 (dashed grey line): water from host rock; CL4 (dashed black line): water from fluorite vein.

comparison of our data with published data on mixite-group minerals from localities worldwide shows that analyzed compositions are in good agreement with the Schwarzwald samples (Fig. 10); no literature data pertain to agardite–mixite solid solutions, which supports our assumption of a miscibility gap between these minerals.

Although goudeyite is the IMA-approved Al end-member of the mixite group (Table 1), we decided to calculate Al at the *M2* site, because Al correlates negatively with Cu + Fe. Its ionic radius (in sixfold coordination, Al^{3+} has a radius of 0.61 Å, Whittaker & Muntus 1970) is much smaller than for other cations ($\text{Bi}^{3+}=1.10$, $\text{La}^{3+}=1.13$, $\text{Ca}^{2+}=1.08$, $\text{Pb}^{2+}=1.26$ Å) at the *M1* site, which makes an Al end-member with mixite structure unlikely. Furthermore, the few published compositions of goudeyite do not perfectly fit the ideal formula (Wise 1987, Moura *et al.* 2007).

Among the samples of agardite, there are La-, Ce-, Nd- and Y-dominant samples. “Agardite-(Dy)”, reported but only incompletely characterized by Walenta (1970), was not found in the course of the present study; its existence is therefore still uncertain.

Furthermore, we show that differences in the concentration of REE are generally very small, and a correct identification is only possible with a precise analysis. The EDX spectra acquired do not suffice to derive correct REE abundances, as peak overlaps can result in a misinterpretation of the spectra. Publications of agardite occurrences with chemical specification in their name, but without precise chemical analytical data, should therefore be regarded cautiously.

Distribution of rare-earth minerals in the Schwarzwald

When taking the geological context into account, a correlation between the geological environment and the distribution of mixite-group minerals can be found (Fig. 4). Samples from the northern Schwarzwald mostly consist of zálesfite with elevated Bi or REE contents or both. It originates in barite veins with Cu–Bi mineralization in sandstones overlying Variscan granites (group 4, after Staude *et al.* 2009). The sandstones were (or still are) covered by limestones, which explains the high Ca contents in these mixite-group minerals. As

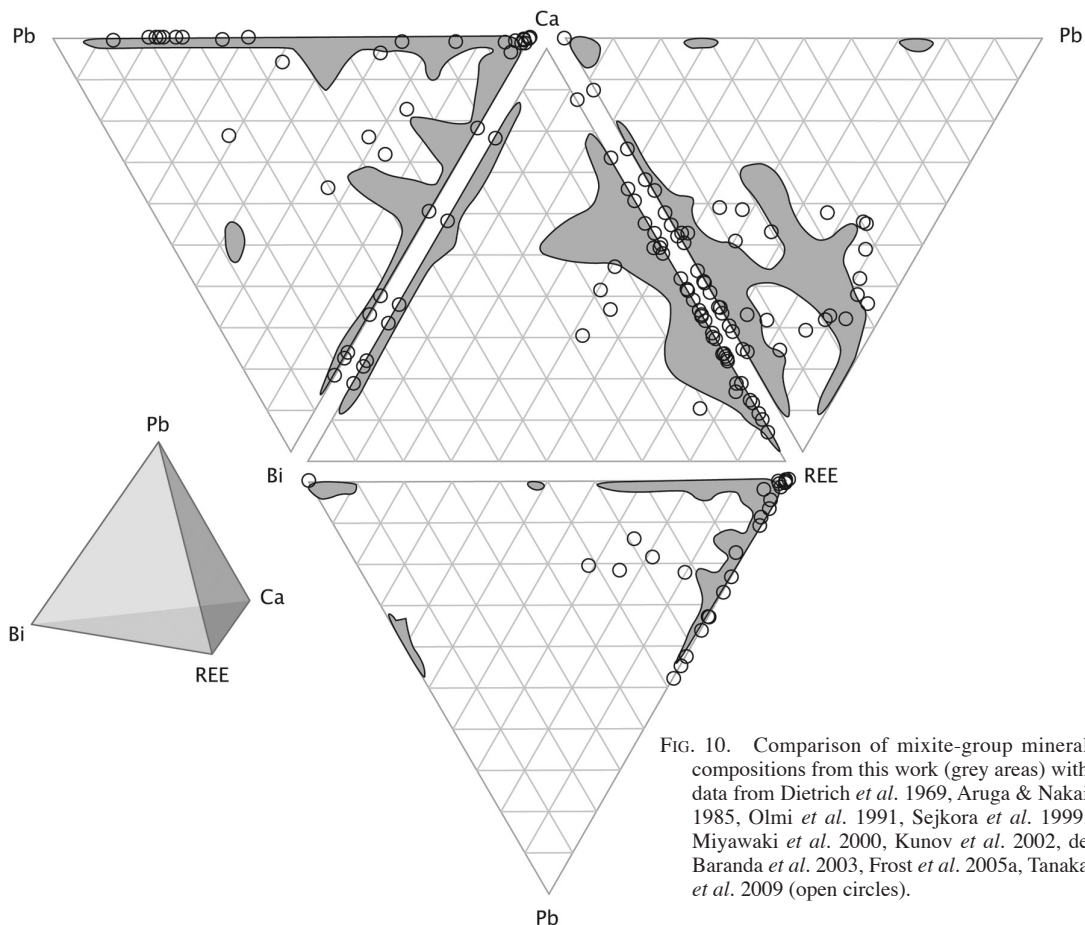


FIG. 10. Comparison of mixite-group mineral compositions from this work (grey areas) with data from Dietrich *et al.* 1969, Aruga & Nakai 1985, Olmi *et al.* 1991, Sejkora *et al.* 1999, Miyawaki *et al.* 2000, Kunov *et al.* 2002, de Baranda *et al.* 2003, Frost *et al.* 2005a, Tanaka *et al.* 2009 (open circles).

the southern Schwarzwald is more deeply eroded, it is not surprising to find less strongly calcic compositions there. The only sample from sandstone-hosted veins, which is related to a fluorite–barite vein (SG168 from Käfersteige, group 2 after Staude *et al.* 2009), is also the only one from the northern Schwarzwald group that is not zálesítite, but rather agardite. Obviously, the REE are here derived from dissolution of fluorite, as is the case in many localities along the NKF (see below) or in the southern Schwarzwald.

Samples from the NKF are mostly agardite–zálesítite solid solutions with only minor amounts of Bi (up to 0.12 *apfu* Bi). However, Pb can reach higher amounts, up to 0.3 *apfu*, which can be explained by the common occurrence of galena in these veins. In contrast to the agardite–zálesítite solid solutions related to the NKF, the Wittichen area shows only mixite–zálesítite solid solutions, although only a few km separates the two districts. Whereas along the NKF, Bi is only present in rare sulfosalts, it occurs as a native element in Wittichen

(Staude *et al.* 2010a, in press). More importantly, however, Bi is much more abundant in Wittichen than along the NKF, and fluorite, a source of the REE, is uncommon in Wittichen compared to the NKF deposits.

In the southern Schwarzwald, most veins contain Pb–Zn mineralization in fluorite – barite – quartz gangue. Accordingly, many of the analyzed samples, which are mostly agardite–zálesítite solid solutions, are Pb-rich. Only the sample from Säckingen (SG201) consists of mixite with a zálesítite component of ~0.3. This sample is from a quartz vein comprising a W–Bi–Cu mineralization, which formed by late-magmatic fluids (Werner *et al.* 1990, Schatz & Otto 1989).

There is a systematic correlation of mixite-group end-members with distinct areas, but it is not obvious why only certain end-members form in certain chemical environments. In Wittichen, for example, no agardite was found in our study (although it has been described as a rare mineral from there; Walenta 1992), despite the occurrence of REE-rich “pitchblende” (Leibiger

1955). In contrast, in the northern Schwarzwald, more REE- than Bi-rich zálesfite formed, although there is no obvious REE source, but Bi-bearing tennantite is common (Staude *et al.* 2010b). It appears that the occurrence of REE-rich mixite-group minerals is not only related to the assemblage and composition of the primary minerals, but also to other factors. Therefore, possible sources and their REE contents have to be considered.

Source of the REE

In the Schwarzwald, the REE are concentrated to the percent level in secondary minerals, mainly arsenates and phosphates, which are the products of supergene alteration of hydrothermal veins. Their REE content can have the following sources:

1) Primary fluorite or carbonate: They contain REE in the ppm range (Schwinn & Markl 2005, Loges *et al.* 2009). The common occurrence of secondary fluorite and carbonate and typical dissolution features in primary gangue minerals attest to the mobilization of REE during weathering of fluorite- and carbonate-bearing veins.

2) Primary “pitchblende”: At Menzenschwand, primary “pitchblende” contains REE in the ppm range (Hofmann 1989); at Wittichen, they even reach concentrations of up to 3 wt.%, with a relative enrichment of the HREE (Leibiger 1955), which can be released during weathering. As “pitchblende” is easily weathered (which can be seen in hand specimen, as it acquires a “spongy” texture) and secondary uranium minerals are common at both localities (whereas fluorite is not), this is a very likely REE source.

3) Host rocks: The host rocks contain relatively REE-rich minerals like apatite or magmatic uraninite (in granites; Hofmann 1989) and REE-poor minerals like feldspars or biotite. Upon alteration, their REE can become at least partly remobilized.

The REE patterns of primary and secondary minerals and the mine waters allow us to discriminate between the three possibilities for the different localities. At localities along the NKF, REE could originate from fluorite and carbonates from the veins or from the host rock. The fluorite (or carbonate) is obviously dissolved and dominates the REE distribution in the water that flows through the vein (Fig. 11a). Primary fluorite (or carbonate) thus is an important REE source in these veins. Furthermore, these data show that water flowing along the fluorite vein of the Clara mine does not contain more REE than the water draining from the host rock. As many examples of secondary fluorite show REE patterns similar to those of the host-rock-derived waters (Fig. 11a), we assume that the host rock contributes significantly to the REE budget in the secondary minerals. A contribution from the host rock is also very likely, as no primary phosphate minerals (but only secondary phosphates) occur in the veins.

This implies that apatite and possibly other minerals from the host rock contribute to the REE content of the mineral-precipitating waters.

In Wittichen, the primary mineralization differs from that along the NKF; as there are different types of mineralization present in Wittichen (Staude *et al.* in press), there are different possible sources of the REE. In the fluorite–barite veins, fluorite could be the dominant REE source. However, in the barite-dominant veins, from which most samples analyzed in this study originate, fluorite or carbonates are rare, and “pitchblende” is a more likely REE source.

At the Menzenschwand uranium deposit, “pitchblende” is very common (Hofmann 1989). The LREE are relatively depleted if the data are normalized to PAAS. As “pitchblende” is very abundant at Menzenschwand, it is reasonable to assume it to be an important REE source, which would also explain the lack of mixite-group minerals and the occurrence of HREE-rich churchite-(Y). The host rock seems to be a source for P, as secondary uranium and REE phosphates are very common in Menzenschwand. In addition, the REE could therefore also originate from apatite and magmatic uraninite (which is also relatively enriched in HREE; Hofmann 1989) from the granitic host-rock.

Comparison of the Schwarzwald deposits to similar deposits where mixite-group minerals occur also

TABLE 10. ANALYTICAL DATA ON WATER

	Neu- bulach	Teufels- grund	Johann Baptist	CL1	CL2	CL3	CL4
pH	8.5	6.6	6.7	7.3	6.7	6.5	6.6
T [°C]	11.1	10.6	9.6	10.7	9.0	15.9	22.7
Li ⁺ ppm	0.01	0.00	0.00	0.00	0.01	0.03	0.01
Na ⁺	3.80	3.96	1.82	2.30	1.80	5.77	6.78
K ⁺	2.09	0.96	1.33	1.12	2.73	3.43	2.79
Mg ²⁺	30.25	3.75	4.34	2.08	3.28	4.87	5.45
Ca ²⁺	72.62	14.01	7.80	8.95	13.54	22.37	22.76
Ba ²⁺	0.38	0.07	0.15	0.26	0.43	0.05	0.11
F ⁻	0.41	2.52	0.02	0.58	0.94	3.30	4.33
Cl ⁻	15.79	1.86	1.07	1.44	1.27	2.41	5.65
Br ⁻	0.02	0.03	b.d.l.	0.01	0.01	0.05	0.10
NO ₃ ⁻	23.24	7.77	3.29	3.21	7.43	5.18	2.12
PO ₄ ³⁻	b.d.l.	b.d.l.	0.36	b.d.l.	b.d.l.	b.d.l.	b.d.l.
SO ₄ ²⁻	13.64	35.63	4.60	12.03	2.44	35.37	32.12
HCO ₃ ⁻	n.a.	n.a.	36.11	n.a.	n.a.	n.a.	n.a.
La	1.6E-06	1.6E-04	8.0E-06	1.8E-05	4.8E-07	2.3E-05	9.7E-07
Ce	6.8E-07	6.1E-05	3.1E-06	2.7E-05	5.9E-07	1.1E-06	1.0E-06
Pr	1.2E-06	3.0E-05	2.0E-06	6.2E-06	7.8E-08	5.4E-06	2.8E-07
Nd	7.3E-06	1.3E-04	1.0E-05	3.0E-05	5.3E-07	2.4E-05	2.0E-06
Sm	3.3E-06	2.9E-05	3.1E-06	9.5E-06	3.0E-07	6.9E-06	1.3E-06
Eu	1.3E-06	1.3E-05	2.0E-06	4.3E-06	2.6E-07	3.5E-06	9.3E-07
Gd	6.3E-06	3.3E-05	4.4E-06	1.1E-05	8.7E-07	8.7E-06	3.3E-06
Tb	1.0E-06	4.5E-06	6.0E-07	1.7E-06	1.2E-07	1.0E-06	4.8E-07
Dy	6.4E-06	2.4E-05	3.7E-06	1.1E-05	1.1E-06	5.0E-06	2.9E-06
Y	5.9E-05	1.5E-04	3.5E-05	6.3E-05	3.0E-05	3.6E-05	4.5E-05
Ho	1.4E-06	4.1E-06	8.3E-07	2.3E-06	3.2E-07	8.4E-07	5.9E-07
Er	4.1E-06	9.5E-06	2.5E-06	6.9E-06	1.0E-06	1.8E-06	1.7E-06
Yb	3.6E-06	5.6E-06	2.4E-06	6.9E-06	8.5E-07	9.7E-07	1.5E-06
Lu	5.2E-07	8.1E-07	3.8E-07	1.1E-06	1.2E-07	1.4E-07	2.1E-07

n.a.: not analyzed; b.d.l.: below detection limit. CL1: water from creek close to the mine entrance; CL2: water from level 8.2, from vein; CL3: water from level 14.2, from the host rock, and CL4: water from level 18, from the vein.

shows that not only the type of primary mineralization determines the chemical composition of the secondary minerals. At the sites of U–Cu–As–Bi–Co mineralization near Dalbeattie, south Scotland, supergene alteration led to the formation of mixite (Braithwaite & Knight 1990). However, at the U–Ni–Co–As–Ag–Bi deposit of Zálesí, Czech Republic, no mixite *sensu stricto* is known, whereas it is the type locality of REE-bearing and Bi-free zálesítite (Sejkora *et al.* 1999).

Agardite investigated in the present study is LREE-dominant and HREE-depleted. This is to be expected because the ionic radii of the LREE³⁺ are much closer to those of Ca²⁺ and Bi³⁺ than to those of the HREE³⁺. However, the U ore in Wittichen is relatively enriched in HREE and strongly depleted in LREE (Leibiger 1955); this might be the reason for the very rare occurrence of agardite at Wittichen (Walenta 1992). The only REE-bearing zálesítite from Wittichen (SG115, Fig. 6g) is relatively more depleted in the LREE than the other samples. The rare occurrence of HREE-dominant xenotime in the vicinity of corroded “pitchblende” from Wittichen (Walenta 1972) agrees with this idea.

In agardite, various REE may be dominant. Whereas in the central Schwarzwald, agardite is mostly Ce-dominant, many samples from the southern Schwarzwald are Y-dominant. Cerium-dominant agardite from the

southern Schwarzwald was only found in the barite–quartz vein of Amalie-Grünern and the carbonate veins from Rotenbach–Feldberg, whereas all agardite samples from the massive fluorite–barite veins are Y-dominant. The Y dominance in agardite from fluorite veins may be related to the higher stability of Y in fluoride complexes (Gramaccioli *et al.* 1999, Loges *et al.* 2011), which can lead to an enrichment of Y in fluorite and, consequently, if REE originate from fluorite, to dominance of Y in agardite. This interpretation is corroborated by the observation that there are some cases of agardite-(Y) along the NKF, where some veins contain abundant fluorite.

It is also interesting to compare the occurrence of rhabdophane and churchite in the Schwarzwald. As the REE patterns of rhabdophane are usually very similar to those of agardite, they seem to fractionate REE in a similar way; both are enriched in LREE. In contrast, churchite from Menzenschwand is enriched in HREE. As churchite is a HREE phosphate (this work, Lottermoser 1990, Onac *et al.* 2005) and rhabdophane contains LREE (this work, Nagy & Draganits 1999, Berger *et al.* 2008), the formation of churchite or rhabdophane is clearly related to the dominance of light or heavy REE, which explains the fact that churchite occurs only in areas without rhabdophane and *vice*

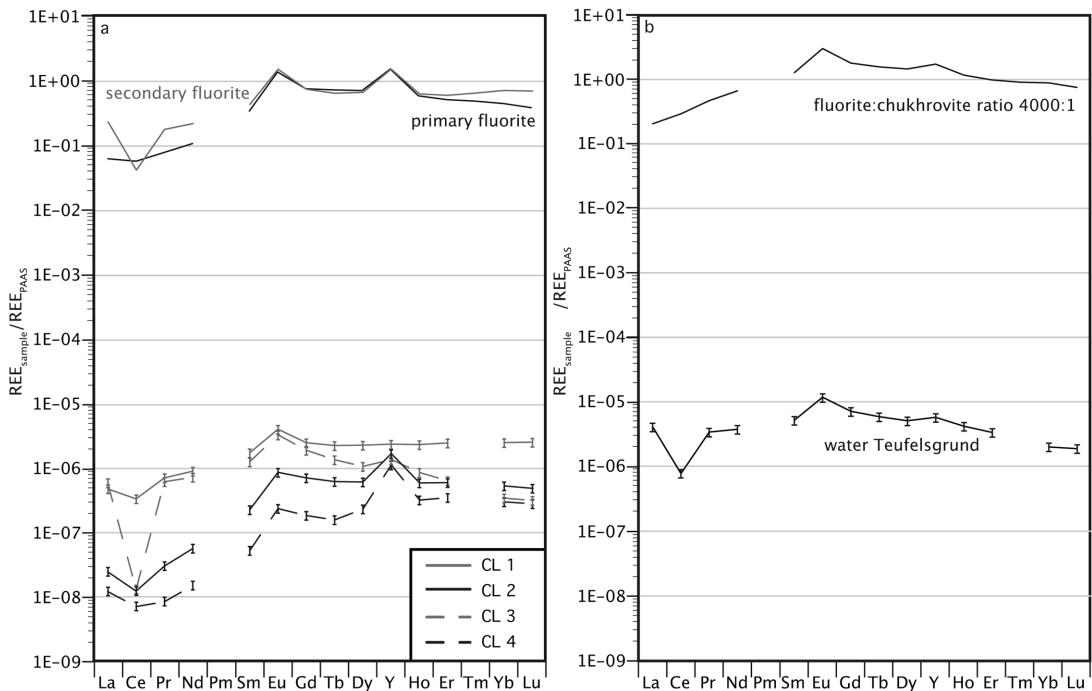


FIG. 11. a) REE patterns for waters from the Clara mine (for legend, see Fig. 9) and mean REE patterns for primary (black line, $n = 86$) and secondary (grey line, $n = 144$) fluorite (all data taken from Loges *et al.* 2009). b) REE pattern for water from Teufelsgrund and calculated REE pattern resulting for a fluorite:chukhrovite ratio of 4000 : 1.

versa. Their occurrence appears to be controlled by the REE makeup of the REE source. The absence of the HREE-preferring secondary mineral churchite in Wittichen is certainly related to the high As:P ratio in the alteration fluids there, which is caused by the abundant occurrence of arsenides at Wittichen.

Anomalies in the REE patterns

The Eu anomalies of the secondary REE minerals are positive in most cases; only the churchite samples from Menzenschwand have a slightly negative Eu anomaly. As Eu fractionation occurs only at temperatures >250°C (Sverjensky 1984, Bau 1991), a Eu anomaly in low-temperature minerals must be inherited from the REE source.

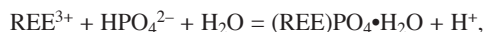
Cerium anomalies are usually not present or only very weakly so; only in some cases are they strongly negative (Fig. 7). Cerium is oxidized at high $f(\text{O}_2)$ and low temperatures, and although inorganic oxidation to Ce^{4+} is a kinetically slow process, it can be mediated by microbial activity (Moffett 1990) or surface catalysis on Mn oxides (e.g., Koepfenkastrof & De Carlo 1992, Bau 1999, Bau & Koschinsky 2009). For mass-balance reasons, the formation of a negative Ce anomaly in a mineral or fluid is invariably related to the formation of a positive Ce anomaly somewhere else in the same system. Oxides and hydroxides of Mn are known to develop strongly positive Ce anomalies and to be the major controlling factor of Ce oxidation (Ohta & Kawabe 2001). Cerianite-(Ce), which was described by Kolitsch *et al.* (2010) from the Clara mine, is another mineral that concentrates Ce, but as it is inconspicuous, it might be overlooked in many cases. If these minerals precipitate, they leave behind water with a negative Ce anomaly, from which minerals with a negative Ce anomaly can precipitate. In this case, the positive and negative Ce anomalies are decoupled. If Mn oxides and REE minerals precipitate concomitantly at the same place, the two Ce anomalies are coupled. Both processes can occur.

Coupled formation of Ce anomalies can be observed in Mn oxides and mixite-group minerals (sample SG52; Figs. 2h, 8c), which shows that formation of Ce anomalies can be a very small-scale process that is defined by the precipitating minerals. Whereas Ce^{4+} is sorbed to Co–Cu-rich Mn^{4+} oxides (resulting in a positive Ce anomaly), the coprecipitating agardite develops a negative Ce anomaly. Interestingly, the Ba-rich Mn oxide parts (which are assumed to incorporate Mn^{3+}) do not show a Ce anomaly, which leads to an inference that Ce fractionation in this case does not take place during transport but during mineral precipitation.

The process resulting in decoupled Ce anomalies is reflected by the REE patterns of agardite (SG205) and the corresponding precipitating water from the Johann Baptist mine. Both display a negative Ce anomaly, suggesting that the Ce anomaly in the agardite is

inherited from the water. Whereas sample SG205 was taken from a wall where water was flowing and mineral precipitation was occurring, samples SG203 and SG204 were taken from a currently dry part of the mine. These two samples do not display a negative Ce anomaly (Fig. 6f), which suggests that there are different generations of secondary minerals related to systems with different fluids. These can be distinguished on the basis of REE mineral compositions.

Whereas the decoupling described above results from the separation of Ce^{4+} from REE^{3+} , a further process is needed to explain the positive Ce anomaly in rhabdophane (e.g., sample SG118; Fig. 12a). Rhabdophane itself incorporates REE^{3+} , which makes a Ce anomaly caused by preferred Ce^{4+} incorporation unlikely. Consequently, a process that separates Ce as Ce^{4+} from the other REE followed by Ce^{4+} reduction to Ce^{3+} is needed to explain the observed anomalies. The complexation of Ce^{4+} with highly selective and highly soluble organic ligands, which preferentially mobilize Ce^{4+} compared to the REE^{3+} (Tanaka *et al.* 2010), presents a way to keep Ce^{4+} in solution. Tanaka *et al.* (2010) demonstrated that the organic Ce^{4+} complexes they observed were not stable at acidic pH, probably because Ce is reduced or ligands are not stable under acidic conditions. Locally decreasing pH could therefore induce the Ce^{4+} complexes to decay and cause Ce to be reduced to Ce^{3+} . As rhabdophane forms according to the reaction



the pH in the fluid close to the surface of the growing rhabdophane decreases, which could then result in a positive Ce anomaly.

The same process can occur if zálesíte precipitates according to the reaction



The fact that one sample of zálesíte (SG79Ch) displays a slightly positive Ce anomaly ($\text{Ce}/\text{Ce}^* = 1.1$ to 1.8) whereas a cogenetic calcite (SG79Ca) shows a negative Ce anomaly ($\text{Ce}/\text{Ce}^* = 0.4$) indicates that Ce liberation and reduction are local processes taking place on the surface of the growing mineral.

Not only Ce, but also all REE^{3+} can be influenced by the coprecipitation of REE minerals with other minerals. To assess this influence, we compared a sample of calcite from Neubulach (SG79Ca), which is cogenetic with zálesíte (SG79Ch), with calcite sinter (SG159) from the same locality, that grew in isolation from other secondary minerals. In addition, water dripping from the sinter was analyzed. If one normalizes the REE in the isolated calcite (SG159) to the water, the observed fractionation is weak and linearly dependent on ionic radius of the REE (Fig. 12b). The other calcite (SG79Ca),

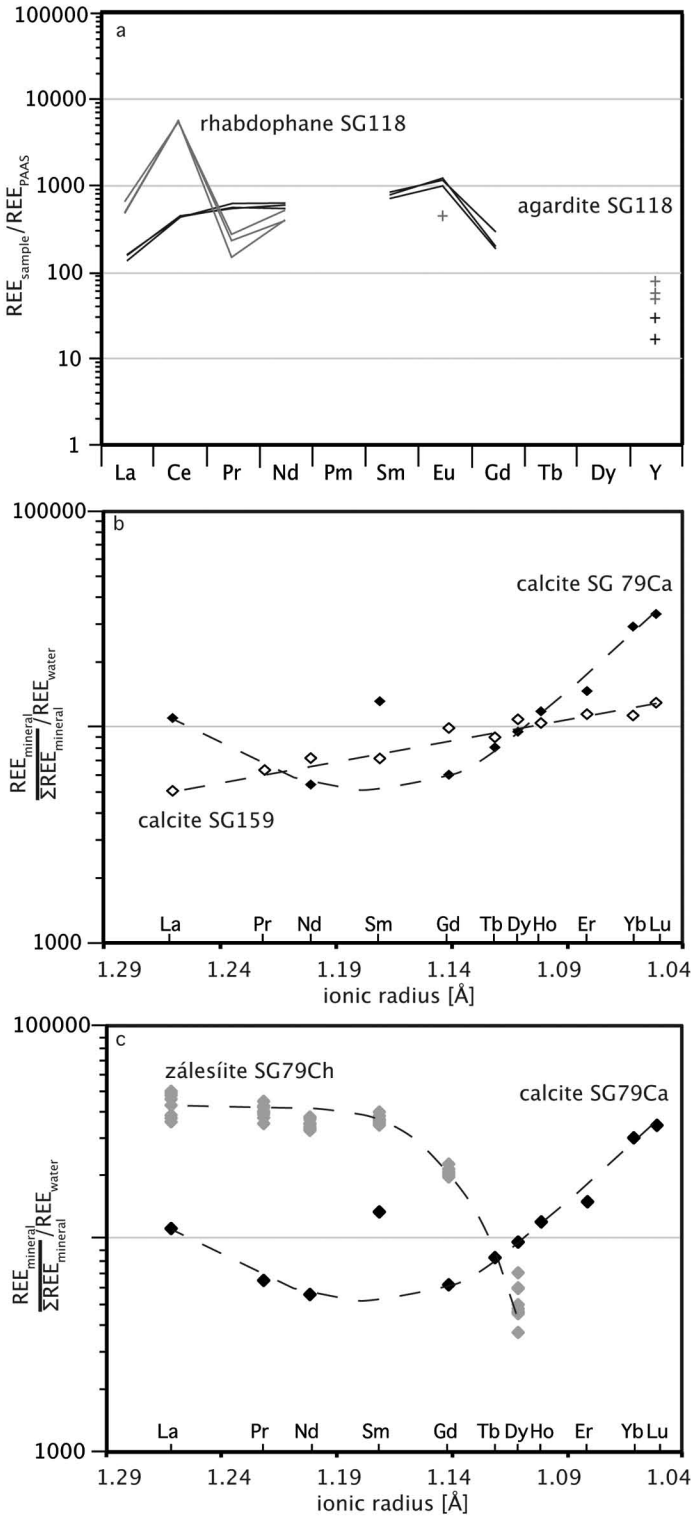


FIG. 12. REE patterns of agardite overgrown by rhabdophane (a). REE patterns from intergrown calcite (SG79Ca) and zálesíite (SG79Ch) and isolated calcite (SG159) normalized to water sampled from Neubulach (b and c).

which is cogenetic with zálesfite, shows a decidedly different and non-linear fractionation with respect to the water. Moreover, the two cogenetic minerals display a complementary fractionation behavior (Fig. 12c). If calcite alone does not show this intense fractionation, it must be caused by the zálesfite. The resulting REE pattern in the water is then imprinted on the calcite.

The cogenetic minerals fluorite (AL31FIII) and chukhrovite (AL31Chk) from Teufelsgrund have clearly different REE patterns (Fig. 8a), although they must have precipitated from the same fluid. Whereas chukhrovite is relatively depleted in HREE, fluorite is relatively depleted in LREE (Fig. 8a). Both show similar Eu anomalies (chukhrovite Eu/Eu^* in the range 2.0 to 2.2 and fluorite Eu/Eu^* in the range 1.7 to 2.9), but very different Y/Ho values (chukhrovite Y/Ho in the range 12.4 to 26.6 and fluorite Y/Ho in the range 27.1 to 108.2). The REE patterns resulting from a combination of different ratios of chukhrovite (AL31Chk-1) and fluorite (AL31FIII-4) show that with a fluorite:chukhrovite ratio of 4000:1, the REE pattern is very close to that of the analyzed water (Fig. 11b; $\text{Eu}/\text{Eu}^* = 1.9$, $\text{Y}/\text{Ho} = 37.4$ and $\text{Gd}/\text{Lu} = 3.8$ for the water and $\text{Eu}/\text{Eu}^* = 2.0$, $\text{Y}/\text{Ho} = 40.4$ and $\text{Gd}/\text{Lu} = 2.4$ for the calculated chukhrovite:fluorite water ratio). Only the La/Sm values 0.8 (water) and 0.2 (fluorite:chukhrovite 4000:1) differ more strongly from each other, which may indicate slight differences in LREE depletion between the water, which precipitated the minerals and the modern water that was analyzed. The modern water also displays a negative Ce anomaly, which is not observed in the fluorite:chukhrovite 4000:1 pattern. This might indicate more oxidizing conditions in the modern water.

SUMMARY AND CONCLUSIONS

In the present study, we report a large dataset of quantitative analyses of secondary rare-earth minerals. For mixite-group minerals, these data show that there is a miscibility gap between mixite and agardite, and that only zálesfite can incorporate small amounts of both Bi and REE. Miscibility between agardite and zálesfite and between mixite and zálesfite is complete. In the Schwarzwald, the Cu arsenates mixite and agardite do not occur at the same locality; neither do the phosphates rhabdophane and churchite. This is probably due to the prevalence of LREE or HREE relative to PAAS. Where LREE are the dominant REE, agardite or rhabdophane form; a prevalence of HREE leads to the formation of churchite, and abundant Bi favors mixite. These differences in the formation of rare-earth minerals are related to differences in the REE source. If fluorite or the gneissic host-rocks are the source, the LREE dominate, and agardite and rhabdophane form. If REE derive from “pitchblende”, the pattern is HREE-dominated, and

churchite can form if P is abundant. In the barite veins in Wittichen, distinct REE minerals are very rare in spite of the high REE contents of the “pitchblende”. This is because As dominates largely over P, and Bi concentrations are high, so that mixite precipitates.

Cerium anomalies can be coupled (positive and negative anomalies occur in adjacent coprecipitating minerals) or decoupled (an anomaly occurs without adjacent complementary anomaly; Fig. 13). Coupled anomalies only develop during precipitation, where Ce^{4+} is preferably incorporated in Mn^{4+} oxides or potentially in cerianite, which results in a negative anomaly in the coprecipitating mineral (Fig. 13a). Decoupled anomalies develop during transport; owing to sorption effects, Ce^{4+} is less mobile than REE^{3+} . This results in a negative Ce anomaly in the fluid, and the precipitated secondary minerals inherit this anomaly (Fig. 13b). However, the formation of organic complexes, which are more stable for Ce^{4+} than for REE^{3+} , can result in a better mobilization of Ce^{4+} . Reduction of Ce^{4+} to Ce^{3+} (possibly due to pH changes) can then lead to positive Ce anomalies in precipitating minerals (Fig. 13c).

The patterns of distribution of REE in cogenetic minerals show that during the formation of secondary minerals, the REE are redistributed. The REE minerals assert a much stronger control over the REE budget and patterns in the water than minerals that incorporate REE only as trace elements and thus influence the REE patterns in coprecipitating minerals like calcite and fluorite. These latter minerals are therefore better suited to reconstruct the original REE profile of the parental water from which they form in the absence of distinct REE minerals. A comparison of texturally related secondary minerals intergrown on the μm scale proves that remobilization and redistribution occur on a very small scale. However, examples of decoupled Ce anomalies show that processes on a larger scale need to be considered as well in order to understand the regional distribution of REE patterns.

ACKNOWLEDGEMENTS

We thank Prof. Dr. Ronald Miletich-Pawliczek (Heidelberg) for providing a crystal of synthetic mixite and for providing useful information on mixite crystallography. Dr. Joachim Gröbner and Prof. Dr. Kurt Walenta provided sample material for analysis. We thank Indra Gill-Kopp for sample preparation, Daniela Meißner and Jule Mawick for ICP-MS measurements, and Dr. Matthias Barth and Antje Huttenlocher for LA-ICP-MS measurements. Dr. Christoph Berthold is thanked for XRD analyses. This research was supported by the Alfred Krupp Prize for Young University Teachers of the Krupp Foundation to G.M. We thank Robert F. Martin, Ru Cheng Wang and an anonymous reviewer for their comments.

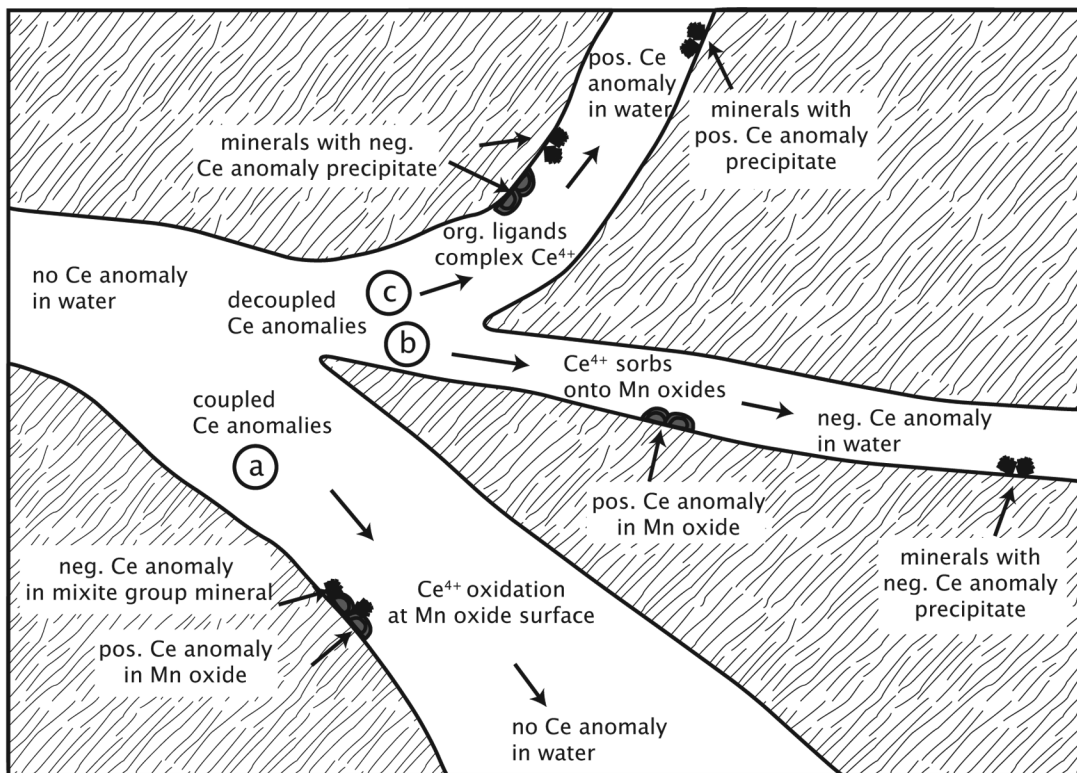


FIG. 13. Sketch showing the possibilities in the formation of a Ce anomaly. As decoupling is influenced by water-rock interaction, decoupled Ce anomalies are more likely in areas with low water:rock ratios, coupled Ce anomalies are more likely in areas with a high water:rock ratio.

REFERENCES

- ALEXANDER, B.W. (2008): Trace element analyses in geological materials using low resolution inductively coupled plasma mass spectrometry (ICPMS). *School of Engineering and Science, Jacobs University Bremen, Tech. Rep.* **18**.
- ARUGA, A. & NAKAI, I. (1985): Structure of Ca-rich agardite, $(\text{Ca}_{0.04}\text{Y}_{0.31}\text{Fe}_{0.09}\text{Ce}_{0.06}\text{La}_{0.04}\text{Nd}_{0.01})\text{Cu}_{6.19}[(\text{AsO}_4)_{2.42}(\text{HAsO}_4)_{0.49}](\text{OH})_{6.38}\cdot 3\text{H}_2\text{O}$. *Acta Crystallogr.* **C41**, 161-163.
- ASSAAOUDI, H., ENNACIRI, A., RULMONT, A. & HARCHARRAS, M. (2000): Gadolinium orthophosphate weinschenkite type and phase change in rare earth orthophosphates. *Phase Transitions* **72**, 1-13.
- BAATARTSOGT, B., SCHWINN, G., WAGNER, T., TAUBALD, H., BEITTE, T. & MARKL, G. (2007): Contrasting paleofluid systems in the continental basement: a fluid inclusion and stable isotope study of hydrothermal vein mineralization, Schwarzwald district, Germany. *Geofluids* **7**, 123-147.
- DE BARANDA, B.S., DEL TANAGO, J.G. & VIÑALS, J. (2003): Secondary minerals of the Mazarrón-Águilas mining district, Murcia Province, Spain. *Mineral. Rec.* **34**, 315-338.
- BAU, M. (1991): Rare-earth element mobility during hydrothermal and metamorphic fluid-rock interaction and the significance of the oxidation state of europium. *Chem. Geol.* **93**, 219-230.
- BAU, M. (1999): Scavenging of dissolved yttrium and rare earths by precipitating iron oxyhydroxide: experimental evidence for Ce oxidation, Y-Ho fractionation, and lanthanide tetrad effect. *Geochim. Cosmochim. Acta* **63**, 67-77.
- BAU, M. & DULSKI, P. (1996): Anthropogenic origin of positive gadolinium anomalies in river waters. *Earth Planet. Sci. Lett.* **143**, 245-255.
- BAU, M. & KOSCHINSKY, A. (2009): Oxidative scavenging of cerium on hydrous Fe oxide: evidence from the distribution of rare earth elements and yttrium between Fe oxides and Mn oxides in hydrothermal ferromanganese crusts. *Geochem. J.* **43**, 37-47.

- BERGER, A., GNOS, E., JANOTS, E., FERNANDEZ, A. & GIESE, J. (2008): Formation and composition of rhabdophane, bastnäsite and hydrated thorium minerals during alteration: implications for geochronology and low-temperature processes. *Chem. Geol.* **254**, 238-248.
- BLIEDTNER, M. & MARTIN, M. (1986): *Erz- und Minerallagerstätten des Mittleren Schwarzwaldes*. LGRB, Freiburg, Germany.
- BRAITHWAITE, R.S.W. & KNIGHT, J.R. (1990): Rare minerals, including several new to Britain, in supergene alteration of U–Cu–As–Bi–Co mineralisation near Dalbeattie, south Scotland. *Mineral. Mag.* **54**, 129-131.
- DIETRICH, J.E., ORLIAC, M. & PERMINGEAT, F. (1969): L'agardite, une nouvelle espèce minérale, et le problème du chlorotile. *Bull. Soc. fr. Minéral. Cristallogr.* **92**, 420-434.
- FROST, R.L., ERICKSON, K.L., WEIER, M.L., MCKINNON, A.R., WILLIAMS, P.A. & LEVERETT, P. (2004): Effect of the lanthanide ionic radius on the Raman spectroscopy of lanthanide agardite minerals. *Spectroscopy* **35**, 961-966.
- FROST, R.L., ERICKSON, K.L., WEIER, M.L., MCKINNON, A.R., WILLIAMS, P.A. & LEVERETT, P. (2005b): Thermal decomposition of agardites (REE)-relationship between dehydroxylation temperature and electronegativity. *Thermochim. Acta* **427**, 167-170.
- FROST, R.L., MCKINNON, A.R., WILLIAMS, P.A., ERICKSON, K.L., WEIER, M.L. & LEVERETT, P. (2005c): Studies of natural and synthetic agardites. *Neues Jahrb. Mineral. Abh.* **181**, 11-20.
- FROST, R.L., WEIER, M., MARTENS, W. & DUONG, L. (2005a): Identification of mixite minerals – an SEM and Raman spectroscopic analysis. *Mineral. Mag.* **69**, 169-177.
- GEYER, O.F. & GWINNER, M.O. (1986): *Geologie von Baden-Württemberg*. Schweizerbart, Stuttgart, Germany.
- GRAMACCIOLI, C.M., DIELLA, V. & DEMARTIN, F. (1999): The role of fluoride complexes in REE geochemistry and the importance of 4f electrons: some examples in minerals. *Eur. J. Mineral.* **11**, 983-992.
- HIKICHI, Y., HUKUO, K. & SHIOKAWA, J. (1978): Syntheses of rare earth orthophosphates. *Bull. Chem. Soc. Japan* **51**, 3545-3646.
- HIKICHI, Y., OTA, T., HATTORI, T. & IMAEDA, T. (1996): Synthesis and thermal reactions of rhabdophane-(Y). *Mineral. J.* **18**, 87-96.
- HIKICHI, Y., SASAKI, T., MURAYAMA, K., NOMURA, T. & MIYAMOTO, M. (1989): Mechanochemical changes of Weinschenkite type $RPO_4 \cdot 2H_2O$ (R= Dy, Y, Er, or Yb) by grinding and thermal reactions of the ground specimens. *J. Am. Ceram. Soc.* **72**, 1073-1076.
- HOFMANN, B. (1989): *Genese, Alteration und rezentes Fliess-System der Uranlagerstätte Krunkelbach (Menzschwand, Südschwarzwald)*. Dissertation, Universität Bern, Switzerland.
- HOFMANN, B. & EIKENBERG, J. (1991): The Krunkelbach Uranium Deposit, Schwarzwald, Germany: correlation of radiometric ages (U–Pb, U–Xe–Kr, K–Ar, ^{230}Th – ^{234}U) with mineralogical stages and fluid inclusions. *Econ. Geol.* **86**, 1031-1049.
- HUCK, K.-H. (1984): *Die Beziehungen zwischen Tektonik und Paragenese unter Berücksichtigung geochemischer Kriterien in der Fluß- und Schwespatgrube „Clara“ bei Oberwolfach/Schwarzwald*. Dissertation, Universität Heidelberg, Germany.
- JACOB, D.E. (2006): High sensitivity analysis of trace element poor geological reference glasses by laser-ablation inductively coupled plasma mass spectrometry (LA–ICP–MS). *Geostand. Geoanal. Res.* **30**, 221-235.
- JOCHUM, K.P. & NEHRING, F. (2006): GeoReM preferred values. http://georem.mpch-mainz.gwdg.de/sample_query_pref.asp.
- KALT, A., ALTHERR, R. & HANEL, M. (2000): The Variscan basement of the Schwarzwald. *Beih. Eur. J. Mineral.* **12**, 1-43.
- KESTEN, D. & WERNER, W. (2006): *Karte der mineralischen Rohstoffe von Baden-Württemberg 1 : 50 000. Blätter L 7561 Freudstadt und L 7518 Rottenburg am Neckar*. LGRB, Freiburg, Germany.
- KOEPPEKASTROP, D. & DE CARLO, E.H. (1992): Sorption of rare-earth elements from seawater onto synthetic mineral particles: an experimental approach. *Chem. Geol.* **95**, 251-263.
- KOLITSCH, U., GRÖBNER, J., BRANDSTÄTTER, F. & BAYERL, R. (2010): Neufunde aus der Grube Clara im mittleren Schwarzwald (IV). *Lapis* **35**(9), 22-27.
- KRAUSE, W., BERNHARDT, H.-J., BLASS, G., EFFENBERGER, H. & GRAF, H.-W. (1997): Hechtsbergite, $\text{Bi}_2\text{O}(\text{OH})(\text{VO}_4)$, a new mineral from the Black Forest, Germany. *Neues Jahrb. Mineral. Monatsh.*, 271-287.
- KRENN, E. & FINGER, F. (2007): Formation of monazite and rhabdophane at the expense of allanite during Alpine low temperature retrogression of metapelitic basement rocks from Crete, Greece: microprobe data and geochronological implications. *Lithos* **95**, 130-147.
- KUNOV, A.Y., NAKOV, R.A. & STANCHEV, C.D. (2002): First agardite-(Y), -(Nd), -(La) find in Bulgaria. *Neues Jahrb. Mineral. Monatsh.*, 107-111.
- LEIBIGER, H. (1955): *Beiträge zur Methodik der Gehaltsbestimmung von Uran und Blei in Uranpecherzen zum Zweck der Altersbestimmung und Beiträge zur analytischen Chemie des Urans im allgemeinen: Untersuchungen über das Vorkommen von seltenen Erden und Thorium in den Uran-Kobalt-Erzen des mittleren Schwarzwalds; Erfahrungen und Untersuchungen über die Trennung und*

- Bestimmung von Blei und Wismut mittels Thionalid*. Dissertation, Universität Freiburg i. Br., Germany.
- LEVINSON, A.A. (1966): A system of nomenclature for rare-earth minerals. *Am. Mineral.* **51**, 152-158.
- LOGES, A., GÖB, S., BARTH, M., BAU, M., WAGNER, T. & MARKL, G. (2009): Remobilization of REE in F-rich, low-temperature environments. *Geochim. Cosmochim. Acta* **73**(13S), A788.
- LOGES, A., MIGDISOV, A.A., WAGNER, T., WILLIAMS-JONES, A.E. & MARKL, G. (2011): Fluoride complexation of yttrium under hydrothermal conditions. *Mineral. Mag.* **75**, 1353 (abstr.).
- LOTTERMOSER, B.G. (1990): Rare-earth element mineralisation within the Mt. Weld carbonatite laterite, Western Australia. *Lithos* **24**, 151-167.
- MARKL, G. & BUCHER, K. (1997): Reduction of Cu^{2+} in mine waters by hydrolysis of ferrous sheet silicates. *Eur. J. Mineral.* **9**, 1227-1235.
- MARKL, G., LAHAYE, Y. & SCHWINN, G. (2006): Copper isotopes as monitors of redox processes in hydrothermal mineralization. *Geochim. Cosmochim. Acta* **70**, 4215-4228.
- METZ, R., RICHTER, M. & SCHÜRENBERG, H. (1957): Die Blei-Zink-Erzgänge des Schwarzwaldes. *Beih. Geol. Jb.* **29**.
- MEYER, M., BROCKAMP, O., CLAUER, N., RENK, A. & ZUTHER, N.M. (2000): Further evidence for a Jurassic mineralizing event in central Europe: K-Ar dating of hydrothermal alteration and fluid inclusion systematics in wall rocks of the Käfersteige fluorite vein deposit in the northern Black Forest, Germany. *Mineral. Deposita* **35**, 754-761.
- MILETICH, R. & ZEMANN, J. (1993): Die Synthese des Minerals Mixit. *Aufschluss* **44**, 17-21.
- MILETICH, R., ZEMANN, J. & NOWAK, M. (1997): Reversible hydration in synthetic mixite, $\text{BiCu}_6(\text{OH})_6(\text{AsO}_4)_3 \cdot n\text{H}_2\text{O}$ ($n \leq 3$): hydration kinetics and crystal chemistry. *Phys. Chem. Minerals* **24**, 411-422.
- MIYAWAKI, R., MATSUBARA, S., YOKOYAMA, K., KATO, A. & IMAI, H. (2000): Agardite-(Y) and associated copper minerals from Setoda, Hiroshima Prefecture, Japan. *Mem. Nat. Sci. Mus., Tokyo* **32**, 19-38.
- MOFFETT, J.W. (1990): Microbially mediated cerium oxidation in sea water. *Nature* **345**, 421-423.
- MÖLLER, P., STOBER, I. & DULSKI, P. (1997): Seltenerdelement-, Yttrium-Gehalte und Bleiisotope in Thermal- und Mineralwässern des Schwarzwaldes. *Grundwasser* **2**, 118-132.
- MOURA, M.A., BOTELHO, N.F. & CARVALHO DE MENDONÇA, F. (2007): The indium-rich sulfides and rare arsenates of the Sn-In-mineralized Mangabeira A-type granite, central Brazil. *Can. Mineral.* **45**, 485-496.
- NAGY, G. & DRAGANITS, E. (1999): Occurrence and mineral-chemistry of monazite and rhabdophane in the Lower and Middle Austroalpine tectonic units of the southern Sopron Hills (Austria). *Mitt. Ges. Geol. Bergbaustud. Österr.* **42**, 21-36.
- NAGY, G., DRAGANITS, E., DEMÉNY, A., PANTÓ, G. & ÁRKAI, P. (2002): Genesis and transformations of monazite, florencite and rhabdophane during medium grade metamorphism: examples from the Sopron Hills, Eastern Alps. *Chem. Geol.* **191**, 25-46.
- OHTA, A. & KAWABE, I. (2001): REE(III) adsorption onto Mn dioxide ($\delta\text{-MnO}_2$) and Fe oxyhydroxide: Ce(III) oxidation by $\delta\text{-MnO}_2$. *Geochim. Cosmochim. Acta* **65**, 695-703.
- OLMI, F., SABELLI, C. & TROSTI FERRONI, R. (1991): A contribution to the crystal chemistry of mixite group minerals from Sardinia (Italy). *Neues Jahrb. Mineral., Monatsh.*, 487-499.
- ONAC, B.P., ETTINGER, K., KEARNS, J. & BALASZ, I.I. (2005): A modern, guano-related occurrence of foggite, $\text{CaAl}(\text{PO}_4)(\text{OH})_2 \cdot \text{H}_2\text{O}$ and churchite-(Y), $\text{YPO}_4 \cdot 2\text{H}_2\text{O}$ in Cioclovina Cave, Romania. *Mineral. Petrol.* **85**, 291-302.
- OTTO, J. (1974): Eine neue Kobalt-Kupfer-Arsen-Silbermineralisation im Kinzigtal (Schwarzwald). *Aufschluss* **25**, 513-524.
- PAUTOV, L.A., BEKENOVA, G.K., KARPENKO, V.Y. & AGAKHANOV, A.A. (2005): Chukhrovite-(Nd), $\text{Ca}_3(\text{Nd,Y})\text{Al}_2(\text{SO}_4)\text{F}_{13} \cdot 12\text{H}_2\text{O}$, a new mineral. *New Data on Minerals* **40**, 5-10.
- PEACOR, D.R. & DUNN, P.J. (1982): Petersite, a REE and phosphate analog of mixite. *Am. Mineral.* **67**, 1039-1042.
- PFAFF, K., HILDEBRANDT, L.H., LEACH, D.L., JACOB, D.E. & MARKL, G. (2010): Formation of the Wiesloch Mississippi Valley-type Zn-Pb-Ag deposit in the extensional setting of the Upper Rhinegraben, SW Germany. *Mineral. Deposita* **45**, 647-666.
- PFAFF, K., ROMER, R.L. & MARKL, G. (2009): Mineralization history of the Schwarzwald ore district: U-Pb ages of ferberite, agate, and pitchblende. *Eur. J. Mineral.* **21**, 817-836.
- SCHATZ, R.H. & OTTO, J. (1989): Neue Wolframmineralisationen bei Bad Säckingen im Südschwarzwald. *Jahrb. geol. Landesamt Baden-Württ.* **31**, 153-170.
- SCHRAUF, A. (1880): Ueber Arsenate von Joachimsthal. *Z. Kristallogr.* **4**, 278-285.
- SCHWINN, G. & MARKL, G. (2005): REE systematics in hydrothermal fluorite. *Chem. Geol.* **216**, 225-248.
- SEJKORA, J., ŘÍDKOŠIL, T. & ŠREIN, V. (1999): Zálesite, a new mineral of the mixite group, from Zálesí, Rychlebské hory Mts., Czech Republic. *Neues Jahrb. Mineral., Abh.* **175**, 105-124.

- STAUDE, S., BONS, P.D. & MARKL, G. (2009): Hydrothermal vein formation by extension-driven dewatering of the middle crust: an example from SW Germany. *Earth Planet. Sci. Lett.* **286**, 387-395.
- STAUDE, S., DORN, A., PFAFF, K. & MARKL, G. (2010a): Assemblages of Ag–Bi sulfosalts and conditions of their formation: the type locality of schapbachite ($\text{Ag}_{0.4}\text{Pb}_{0.2}\text{Bi}_{0.4}\text{S}$) and neighboring mines in the Schwarzwald ore district, southern Germany. *Can. Mineral.* **48**, 448-467.
- STAUDE, S., MORDHORST, T., NEUMANN, R., PREBECK, W. & MARKL, G. (2010b): Compositional variation of the tennantite–tetrahedrite solid-solution series in the Schwarzwald ore district (SW Germany): the role of mineralizing processes and fluid source. *Mineral. Mag.* **74**, 309-338.
- STAUDE, S., WAGNER, T. & MARKL, G. (2007): Mineralogy, mineral compositions and fluid evolution at the Wenzel hydrothermal deposit, southern Germany: implications for the formation of Kongsberg-type silver deposits. *Can. Mineral.* **45**, 1147-1176.
- STAUDE, S., WERNER, W., MORDHORST, T., WEMMER, K., JACOB, D.E. & MARKL, G. (in press): The complex multi-stage Co–Ag–Bi–U and Cu–Bi hydrothermal mineralization at Wittichen, Schwarzwald, SW Germany: ore mineralogy, geological setting and conditions of formation. *Mineral. Deposita* DOI 10.1007/s00126-011-0365-4.
- SVERJENSKY, D.A. (1984): Europium redox equilibria in aqueous solution. *Earth Planet. Sci. Lett.* **67**, 70-78.
- TANAKA, K., TANI, Y., TAKAHASHI, Y., TANIMIZU, M., SUZUKI, Y., KOZAI, N. & OHNUKI, T. (2010): A specific Ce oxidation process during sorption of rare earth elements on biogenic Mn oxide produced by *Acremonium* sp. strain KR21–2. *Geochim. Cosmochim. Acta* **74**, 5463-5477.
- TANAKA, T., MINAKAWA, T., KUSACHI, I. & TANABE, M. (2009): Bi-bearing and REE-free zálesite from the Fuka mine, Okayama Prefecture, Japan. *J. Mineral. Petrol. Sci.* **104**, 164-167.
- TAYLOR, S.R. & MCLENNAN, S.M. (1985): *The Continental Crust. Its Composition and Evolution; an Examination of the Geochemical Record Preserved in Sedimentary Rock*. Blackwell, Oxford, U.K.
- WALENTA, K. (1960): Chlorotil und Mixit. *Neues Jahrb. Mineral., Monatsh.*, 223-236.
- WALENTA, K. (1970): Mineralien der Chlorotil-Mixitgruppe mit seltenen Erden von Fundorten im Schwarzwald. *Chem. Erde*, **29**, 36-47.
- WALENTA, K. (1972): Die Sekundärminerale der Co–Ni–Ag–Bi–U-Erzgänge im Gebiet von Wittichen im mittleren Schwarzwald. *Aufschluss* **23**, 279-329.
- WALENTA, K. (1979): Chukhrovit-(Ce) und Rhabdophan-(Ce) aus der Grube Clara im mittleren Schwarzwald. *Chem. Erde* **38**, 331-39.
- WALENTA, K. (1982): Weitere Untersuchungen über das Vorkommen von Selten-Erd-Mineralien im Schwarzwald. *Aufschluss* **33**, 453-458.
- WALENTA, K. (1989): Neufunde aus dem Schwarzwald (3. Folge). *Lapis* **14**(5), 30-37.
- WALENTA, K. (1992): *Die Mineralien des Schwarzwaldes und ihre Fundstellen*. Weise, München, Germany.
- WALENTA, K. (2003): Bleihaltiger Agardit-(Y) von der Grube Silberbrünne bei Gengenbach im mittleren Schwarzwald. *Der Erzgräber* **17**, 39-43.
- WALENTA, K. (2004): Agardit-(Ce) von der Grube Clara im mittleren Schwarzwald. *Aufschluss* **55**, 17-23.
- WALENTA, K. & THEYE, T. (2005): Plumboagardite, a new mineral of the mixite group from an occurrence in the southern Black Forest, Germany. *Neues Jahrb. Mineral., Abh.* **181**, 219-222.
- WALENTA, K. & THEYE, T. (2011): Churchit-(Y) von der Uranlagerstätte Mezenschwand im südlichen Schwarzwald. *Der Erzgräber* **25**, 66-67.
- WERNER, W., SCHLAEGEL, P., BLAUT, P. & RIEKEN, R. (1990): Verbreitung und Ausbildung von Wolframmineralisationen im Kristallin des Schwarzwaldes. *Jahrb. geol. Landesamt Baden-Württ.* **32**, 17-61.
- WHITTAKER, E.J.W. & MUNTUS, R. (1970): Ionic radii for use in geochemistry. *Geochim. Cosmochim. Acta* **34**, 945-956.
- WISE, W.S. (1978): Parnauite and goudeyite, two new copper arsenate minerals from the Majuba Hill mine, Pershing County, Nevada. *Am. Mineral.* **63**, 704-708.
- ZAMBEZI, P., VONCKEN, J.H.L., HALE, M. & TOURET, J.L.R. (1997): Bastnäsite-(Ce) at the Nkombwa Hill carbonate complex, Isoka District, northeast Zambia. *Mineral. Petrol.* **59**, 239-250.

Received June 3, 2011, revised manuscript accepted October 13, 2011.

